AD-A047 044 STANFORD RESEARCH INST MENLO PARK CALIF F/G 17/2.1
INVESTIGATION OF THE USE OF FREQUENCY-DIVISION MULTIPLE ACCESS --ETC(U)
DEC 73 P C JAIN, V E HATFIELD, J K LEUNG DCA100-72-C-0033
UNCLASSIFIED NL

1 OF 2
ADA047044

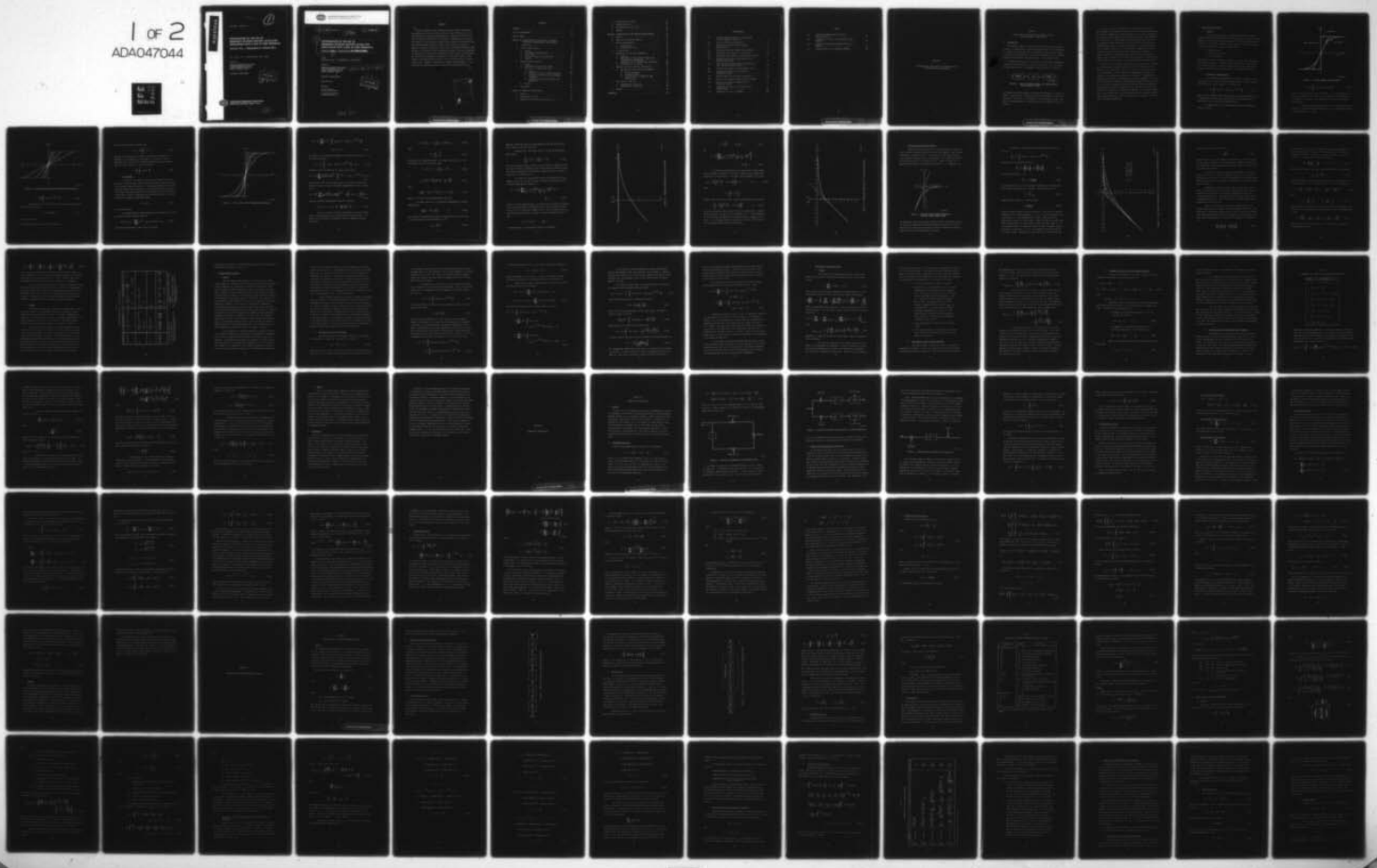

Final Report – Volume Two

INVESTIGATION OF THE USE OF FREQUENCY-DIVISION MULTIPLE ACCESS FOR APPLICATION WITH A MIX OF USER TERMINALS

Volume Two – Appendices to Volume One

By: PRAVIN C. JAIN V. ELAINE HATFIELD JOHN K. LEUNG

Prepared for:

DEFENSE COMMUNICATIONS AGENCY
SYSTEM ENGINEERING FACILITY
DEREY ENGINEERING BUILDING
RESTON, VIRGINIA 22070

CONTRACT DCA100-72-C-0033

STANFORD RESEARCH INSTITUTE
Menlo Park, California 94025 · U.S.A.

STANFORD RESEARCH INSTITUTE
Menlo Park, California 94025 · U.S.A.

(9) Final Report, Volume Two

(12) 106p.

(11) December 1973

(6)

INVESTIGATION OF THE USE OF FREQUENCY-DIVISION MULTIPLE ACCESS FOR APPLICATION WITH A MIX OF USER TERMINALS.

Volume Two – Appendices, ~~to Volume One~~.

II.

(10) By: PRAVIN C. JAIN V. ELAINE HATFIELD JOHN K. LEUNG

Prepared for:

DEFENSE COMMUNICATIONS AGENCY
SYSTEM ENGINEERING FACILITY
DEREY ENGINEERING BUILDING
RESTON, VIRGINIA 22070

(15) DCA100-72-C-0033

CONTRACT DCA100-72-0033

SRI Project 1975

Approved by:

R. F. DALY, *Director*
Telecommunications Department

E. J. MOORE, *Executive Director*
Engineering Systems Division

ABSTRACT

Volume Two comprises three appendices giving detailed analyses of the problem areas in the investigation of the use of FDMA with a mix of user terminals of differing characteristics. Appendix A deals with the limiter transfer characteristic and provides a comprehensive theoretical investigation of the problem of transmitting a number of constant-envelope, phase-modulated FDMA carriers through a limiting satellite repeater. Appendix B analyzes the problem of detection of quadriphase-modulated FDMA carriers at the receiver after transmission through a limiting transponder. An expression for the bit-error probability at the output of an FDMA channel is obtained considering the presence of other FDMA carriers, cross products, and retransmitted up-link as well as down-link noise at the receiver input. Appendix C describes the computer program SYSCON. It also discusses the equations and subroutines used in system optimization.

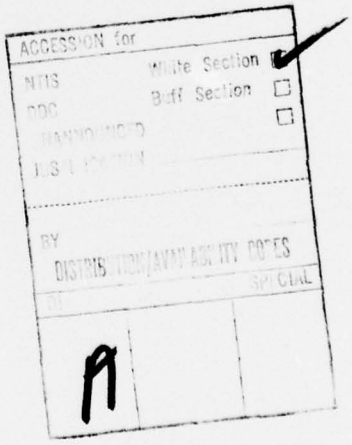

CONTENTS

ILLUSTRATIONS

TABLES

Appendix A

INVESTIGATION OF THE EFFECTS OF BANDPASS LIMITING ON TRANSMISSION OF FDMA SIGNALS

Appendix A

INVESTIGATION OF THE EFFECTS OF BANDPASS LIMITING ON TRANSMISSION OF FDMA SIGNALS

1. Introduction

This appendix documents the results of the investigation performed to provide a comprehensive, theoretical understanding of the transmission of a number of constant-envelope, phase-modulated FDMA carriers through a limiting satellite repeater, and to obtain expressions for the signals, intermodulation products, and up-link noise at the repeater output.

The model generally used in theoretical investigations to represent a limiting satellite repeater is shown in Figure A-1. The limiting can be either hard or soft. The bandpass filter preceding the limiter is

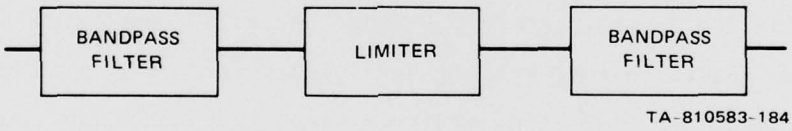

FIGURE A-1 SATELLITE REPEATER MODEL FOR INVESTIGATION OF IDEAL SYMMETRIC LIMITING

wide enough to pass the signals with negligible distortion; it limits the repeater input noise to a bandwidth that is small compared to the center frequency of the filter. The bandpass filter following the limiter confines the output spectrum to essentially only the fundamental band of the signals.

The model of Figure A-1 requires an "ideal" zonal filter at the limiter output, which passes the fundamental band of signals unattenuated but completely suppresses the higher harmonics of the signal frequencies. Real filters can only approximate this desired behavior. The assumption (in Figure A-1) of an ideal bandpass filter following the limiter neglects principally the in-band effects of the filter on the signals, the intermodulation products, and the noise present at the limiter output. However, complete analysis of a more realistic bandpass filter would be extremely difficult, since the system is nonlinear with memory. A rigorous analysis of the problem would involve solving for the filter output, which is related to the limiter input process by a nonlinear differential equation determined by the limiter and filter characteristics.

Section 2 of this appendix develops analytical expressions to represent the nonlinear transfer characteristics for the various types of limiters (e.g., quasi-linear, soft, and hard) that would be of interest in an FDMA system. Section 3 provides a comprehensive, theoretical analysis of the bandpass limiter model of Figure A-1. Expressions for determining the signal, intermodulation, and noise components at the output of the satellite repeater are developed by assuming the input to consist of a sum of n signals of arbitrary amplitude and phase modulation. The analysis is conducted completely in the time domain, to retain the phases of the signals and intermodulation products at the limiter output. This is not possible with the autocorrelation function approach normally used in limiter analysis. Section 4 summarizes the results of Sections 2 and 3 and offers conclusions.

2. Limiter Characteristics

a. General

To analyze the problem of transmitting a number of constant-envelope, phase-modulated sinusoidal carriers through a limiting satellite repeater, we need a mathematical representation for the nonlinear characteristic of the limiter. Generally, three types of limiter characteristics are of interest in satellite communications:

- Hard-limiting
- Quasi-linear-limiting
- Soft-limiting.

These characteristics are shown in Figure A-2. In the hard-limiting case, the output is either $\pm\alpha$. The quasi-linear limiter has a linear region with a sharp break at the saturation point, while a soft limiter has a gradual transition from the linear region to the saturation region.

b. Mathematical Representation

The mathematical representation for each of the three limiter characteristics in Figure A-2 may be obtained from an infinite integral that relates the limiter output y to its input x as

$$y = \frac{2}{\pi} n \int_0^\infty \sin(vx) \cdot \sin(v\alpha/n)\, e^{-v^2\gamma^2/2} \frac{dv}{v^2} \quad , \qquad \text{(A-1)}$$

where α is the constant output limiting level, and the parameters n and γ, respectively, determine how fast saturation is approached with a quasi-linear- and a soft-limiting characteristic.

The characteristic of a quasi-linear limiter is expressed in analytical form as

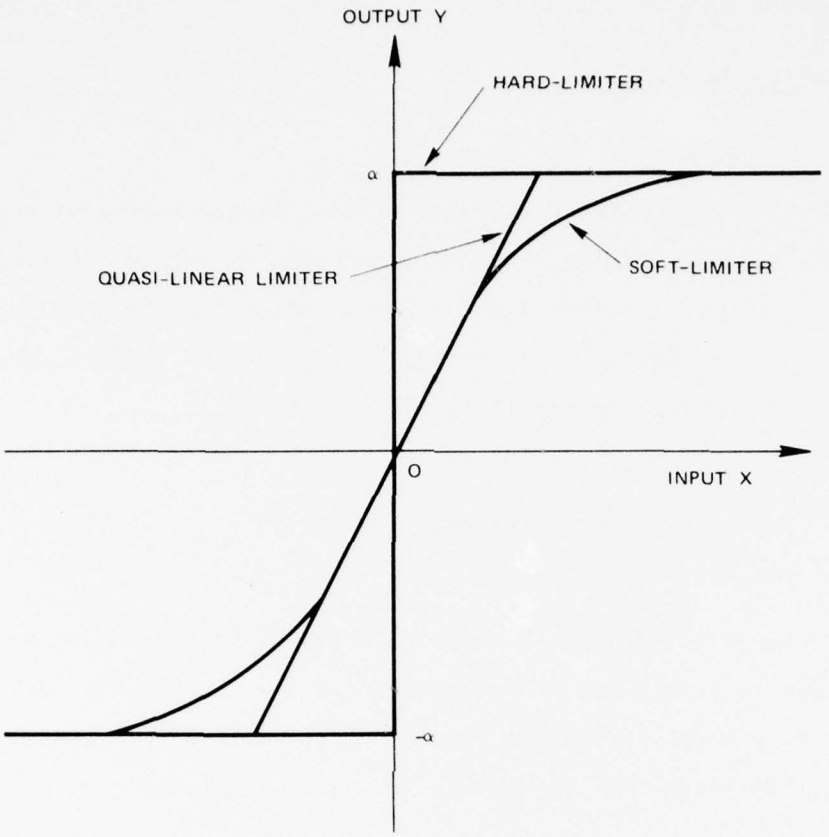

FIGURE A-2 LIMITER TRANSFER CHARACTERISTICS

$$y = \frac{2}{\pi} n \int_0^\infty \sin(vx) \cdot \sin(v\alpha/n) \frac{dv}{v^2} \quad , \qquad (A\text{-}2)$$

which is obtained from Eq. (A-1) by setting $\gamma = 0$. Equation (A-2) is plotted in Figure A-3 and shows how fast saturation is approached as n is increased. For large n, the quasi-linear characteristic becomes hard-limiting.

A soft limiter is usually described by an error-function characteristic. This may be obtained from Eq. (A-1), if n approaches infinity so that $\sin(v\alpha/n) \approx v\alpha/n$, and

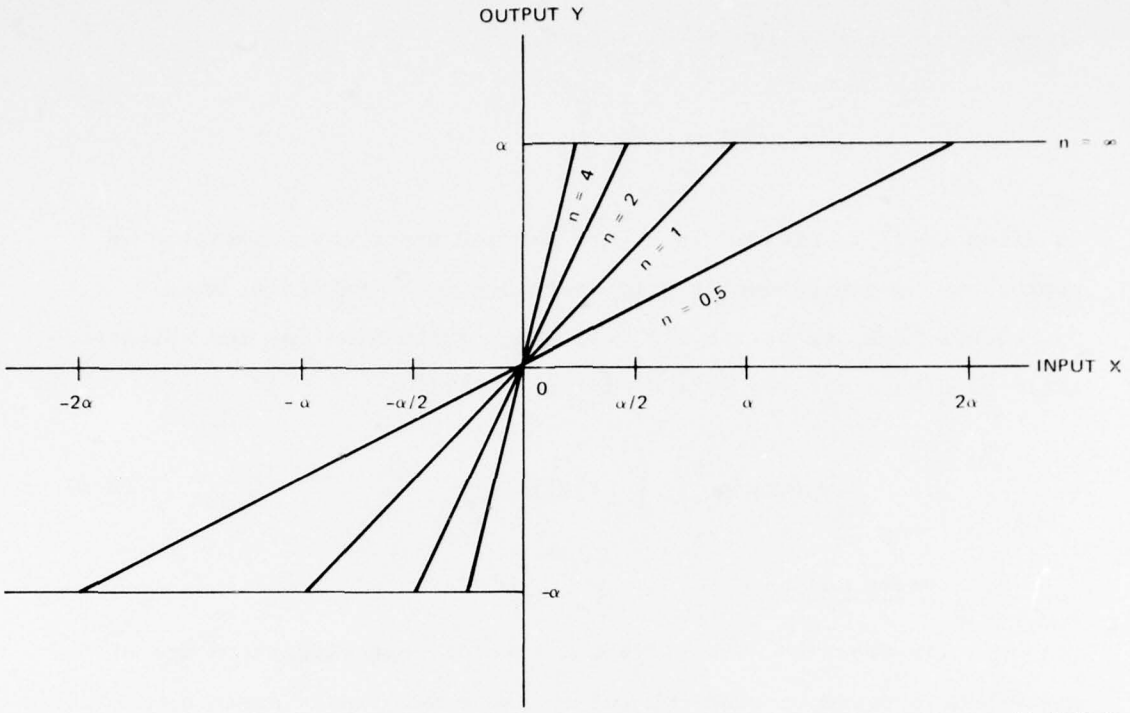

FIGURE A-3 QUASI-LINEAR LIMITER VOLTAGE TRANSFER CHARACTERISTIC

$$y = \frac{2\alpha}{\pi} \int_0^\infty \sin(vx)\, e^{-v^2\gamma^2/2}\, \frac{dv}{v} \quad . \qquad \text{(A-3)}$$

Integration of Eq. (A-3) yields the following more conventional form for soft limiting:[1]*

$$y = \alpha\, \mathrm{erf}(x/\sqrt{2}\gamma) \quad , \qquad \text{(A-4)}$$

---

*References are listed at the end of Volume Two.

where the error function is defined as:

$$\text{erf } z = \frac{2}{\sqrt{\pi}} \int_0^z e^{-t^2} \, dt \quad . \tag{A-5}$$

Equation (A-4) is plotted in Figure A-4 and shows how saturation is approached as the parameter γ is decreased. In the limit, when γ approaches zero, we obtain the well-known expression for the characteristic of a hard limiter [$\gamma = 0$, in Eq. (A-3)]:

$$y = \frac{2\alpha}{\pi} \int_0^\infty \sin(v\cdot) \, \frac{dv}{v} \quad . \tag{A-6}$$

c. Power Output

In practice, the different limiter characteristics are often described in terms of power output versus power input, assuming the input to be a single sinusoidal carrier. It is therefore important to know how the power output-input characteristic can be obtained analytically from the voltage output-input characteristic described above for the different limiter types. Below, we determine the output power for the three types of limiter by assuming a sinusoidal signal

$$x = a \cos \omega t \tag{A-7}$$

at the limiter input.

By substituting the above expression for the signal in Eq. (A-1) and using the Bessel function identity

$$\sin(z \cos \theta) = 2 \sum_{m=0}^{\infty} (-1)^m \cdot J_{2m+1}(z) \cos(2m + 1) \theta \quad , \tag{A-8}$$

the following expression is obtained for the output:

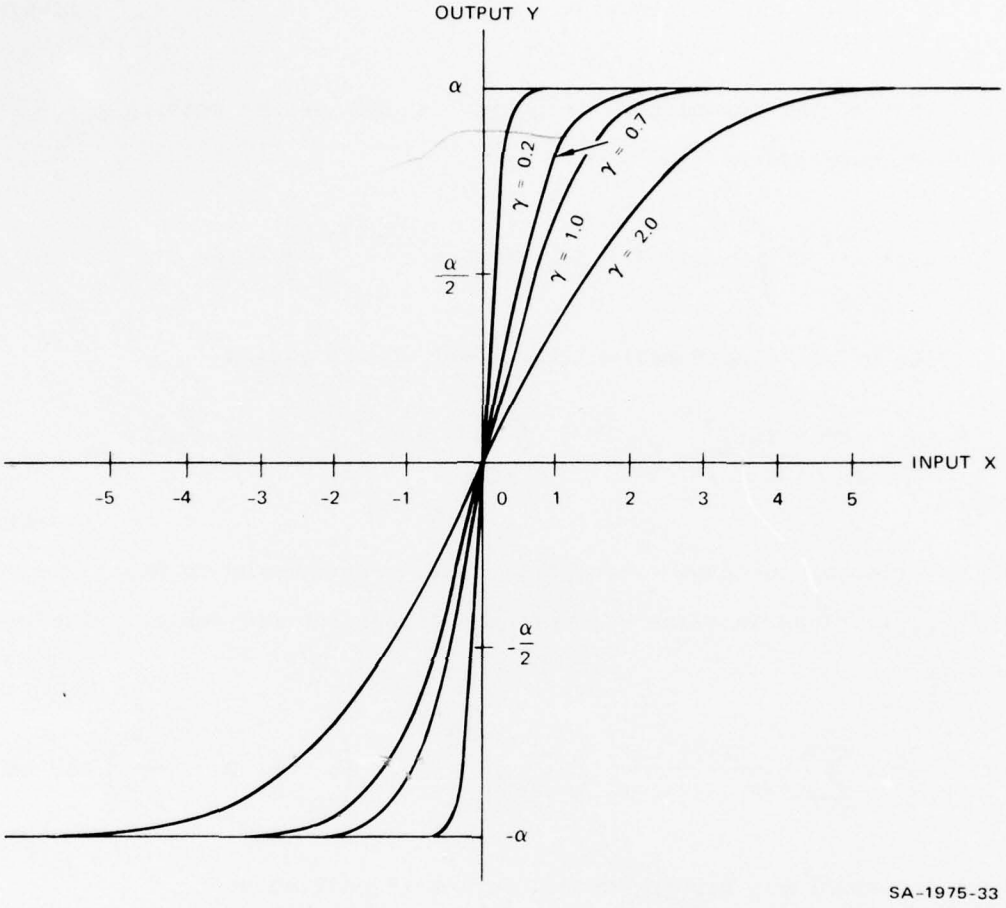

FIGURE A-4 SOFT-LIMITER VOLTAGE TRANSFER CHARACTERISTIC

$$y(t) = \frac{4}{\pi} n \sum_{m=o}^{\infty} (-1)^m \cdot \int_o^{\infty} J_{2m+1}(va) \cdot \sin(v\alpha/n)\, e^{-v^2\gamma^2/2} \frac{dv}{v^2} \quad ,$$

$$\cos(2m + 1)\, \omega t \quad . \qquad \text{(A-9)}$$

The output at the fundamental frequency is obtained by setting m = o in the above expression:

$$g(t) = \frac{4}{\pi} n \int_o^{\infty} J_1(va) \cdot \sin(v\alpha/n)\, e^{-v^2\gamma^2/2} \frac{dv}{v^2} \cdot \cos \omega t \quad . \qquad \text{(A-10)}$$

Expansion of the sine function in a power series yields:

$$g(t) = \frac{4}{\pi} n \sum_{p=o}^{\infty} \frac{(-1)^p}{(2p + 1)!} \left(\frac{\alpha}{n}\right)^{2p+1} \int_o^{\infty} v^{2p-1} \cdot J_1(va) \cdot e^{-v^2\gamma^2/2}\, dv \cos \omega t \quad . \qquad \text{(A-11)}$$

The solution of the above integral, which is attributed to Weber and Sonine,[2] is given in terms of confluent hypergeometric series. The result is:

$$g(t) = \frac{2n}{\sqrt{\pi}} a \sum_{p=o}^{\infty} \frac{(-1)^p}{(2p + 1) \cdot p!} \left(\frac{\alpha}{\sqrt{2}n\gamma}\right)^{2p+1} \cdot {}_1F_1\left(p + \frac{1}{2},\ 2,\ -\frac{a^2}{2\gamma^2}\right) \cos \omega t \quad , \qquad \text{(A-12)}$$

where the confluent hypergeometric series is defined as

$${}_1F_1(a,\ b,\ z) = 1 + \frac{a}{b} \cdot \frac{z}{1!} + \frac{a(a + 1)}{b(b + 1)} \cdot \frac{z^2}{2!} + \ldots \quad . \qquad \text{(A-13)}$$

From Eq. (A-12) we can obtain the output of each of the three limiter characteristics and can also calculate the power output. The output of a soft limiter is obtained by letting n approach infinity. This yields:

$$g(t) = \frac{2}{\sqrt{\pi}} \alpha \cdot \rho \cdot {}_1F_1\left(\frac{1}{2},\ 2,\ -\rho^2\right) \cos \omega t \quad , \tag{A-14}$$

where

$$\rho^2 = \frac{a^2}{2\gamma^2} = \frac{P_i}{\gamma^2} \quad . \tag{A-15}$$

The power of the sinusoidal signal at the input is given by P_i. The power output of a soft limiter is, thus,

$$P_o = \frac{2}{\pi} \alpha^2 \cdot \rho^2 \cdot {}_1F_1^2\left(\frac{1}{2},\ 2,\ -\rho^2\right) \quad , \tag{A-16}$$

or

$$P_o = \frac{2}{\pi} \alpha^2 \rho^2 \, e^{-\rho^2} \left[I_o\left(\rho^2/2\right) + I_1\left(\rho^2/2\right)\right]^2 \quad , \tag{A-17}$$

since

$${}_1F_1\left(\frac{1}{2},\ 2,\ -z\right) = e^{-z/2}\left[I_o(z/2) + I_1(z/2)\right] \quad , \tag{A-18}$$

where $I_o(\ )$ and $I_1(\ )$ are modified Bessel functions.

For large values of ρ^2, the confluent hypergeometric function simplifies to[3]

$${}_1F_1\left(\frac{1}{2},\ 2,\ -\rho^2\right) \approx \frac{2}{\sqrt{\pi}} \frac{1}{\rho} \quad , \quad \rho \to \infty \quad , \tag{A-19}$$

and we obtain the maximum power output in saturation, which is the same as the power output for hard limiting ($\gamma = 0$):

$$P_{max} = \frac{8}{\pi^2} \alpha^2 \quad . \tag{A-20}$$

Equation (A-20) also shows the relationship between the hard-limiting power output and the limiting level.

Combining Eqs. (A-16) and (A-20), we obtain the normalized power output

$$\frac{P_o}{P_{max}} = \frac{\pi}{4} \rho^2 \cdot {}_1F_1^2\left(\frac{1}{2},\ 2,\ -\rho^2\right) \qquad \text{(A-21)}$$

for a soft limiter relative to that for a hard limiter. Equation (A-21) can also be viewed as representing the output power loss resulting from soft limiting compared to hard limiting. Equation (A-21) is plotted in Figure A-5 as a function of ρ^2.

The output of a quasi-linear limiter is obtained by letting γ approach zero in Eq. (A-12) and using the asymptotic expansion for the confluent hypergeometric function:[3]

$$g(t) = \frac{2}{\sqrt{\pi}} \alpha \sum_{p=o}^{\infty} \frac{(-1)^p}{(2p+1) \cdot p! \cdot \Gamma\left(\frac{3}{2} - p\right)} \cdot \left(\frac{\alpha}{na}\right)^{2p} \cos \omega t \quad ,$$

$$\frac{\alpha}{na} \leq 1 \quad , \qquad \text{(A-22)}$$

where $\Gamma(\ )$ is the gamma function. The series in Eq. (A-22) is convergent, as can be easily shown by d'Alembert's ratio test for absolute convergence, if α/na is less than or equal to one. For α/na greater than one, the limiter characteristic, of course, is linear (Figure A-3), and we have

$$g(t) = na \cos \omega t \quad , \quad \frac{\alpha}{na} \geq 1 \quad .$$

The output power of a quasi-linear limiter is, therefore,

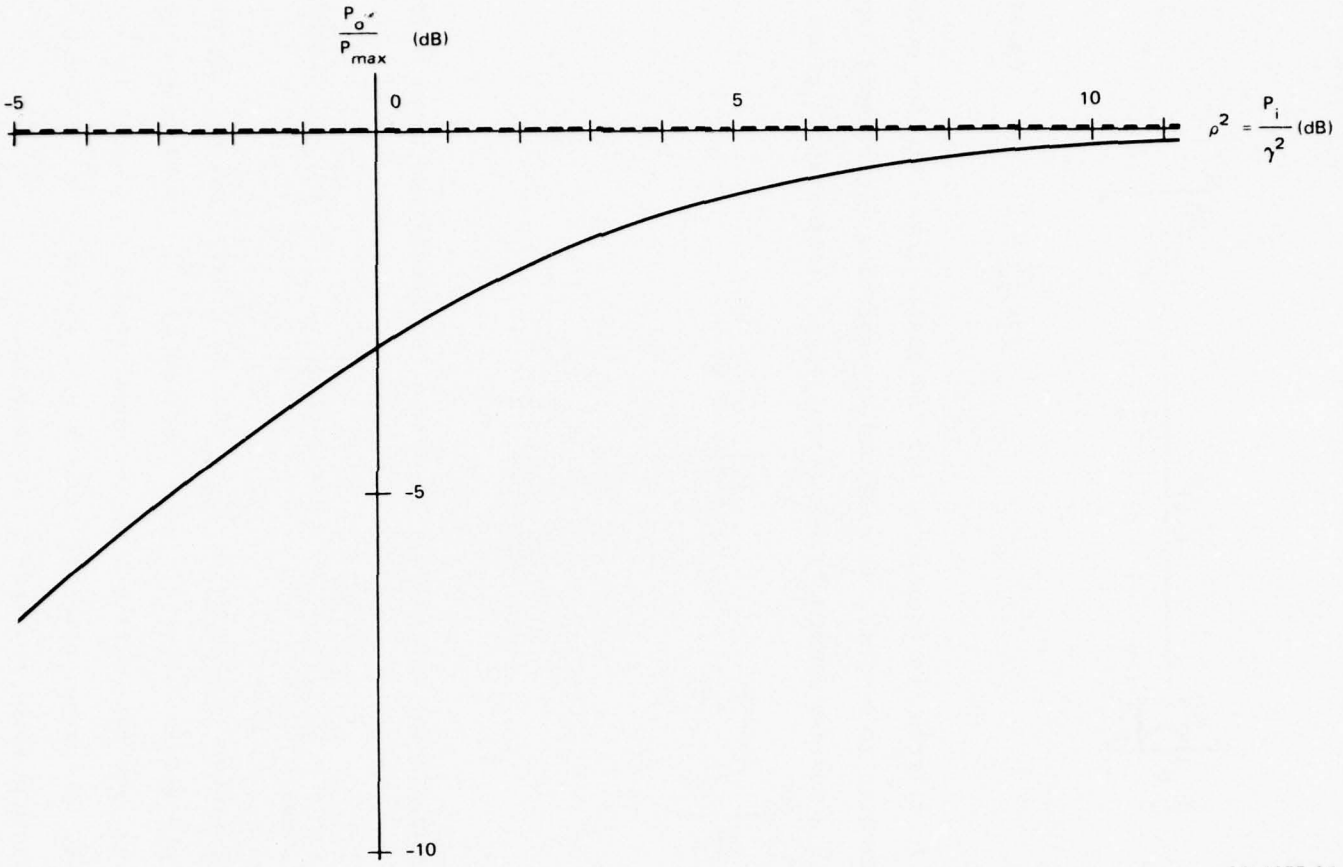

FIGURE A-5 NORMALIZED POWER OUTPUT OF A SOFT LIMITER

$$P_o = \frac{n^2 a^2}{2} \quad , \qquad \text{for } \frac{\alpha}{na} \geq 1 \quad . \tag{A-23}$$

and

$$P_o = \frac{2}{\pi} \alpha^2 \left[\sum_{p=o}^{\infty} \frac{(-1)^p}{(2p+1) \cdot p! \cdot \Gamma\left(\frac{3}{2} - p\right)} \cdot \left(\frac{\alpha}{na}\right)^{2p} \right]^2 \quad ,$$

$$\text{for } \frac{\alpha}{na} \leq 1 \quad . \tag{A-24}$$

An alternative expression for the quasi-linear limiter output, which is simpler to compute, is obtained by expanding the clipped input waveform in a Fourier series.[4] The output signal component is given by:

$$g(t) = \frac{2\alpha}{\pi} \left[\sqrt{1 - \frac{1}{\rho^2}} + \rho \arcsin\left(\frac{1}{\rho}\right) \right] \cos \omega t \quad , \qquad \text{for } \rho \geq 1 \quad , \tag{A-25}$$

where

$$\rho^2 = \frac{n^2 a^2}{\alpha^2} = 2n^2 \frac{P_i}{\alpha^2} \quad .$$

Combining Eqs. (A-25) and (A-20), we obtain the normalized power output:

$$\frac{P_o}{P_{max}} = \frac{1}{4} \left[\sqrt{1 - \frac{1}{\rho^2}} + \rho \arcsin\left(\frac{1}{\rho}\right) \right]^2 \quad , \qquad \rho \geq 1 \tag{A-26}$$

for a quasi-linear limiter relative to that of a hard limiter. Equation (A-26) is plotted in Figure A-6 as a function of ρ^2. It is interesting to note that when the amplitude of the input signal a is equal to α/n, i.e., $\rho = 1$, the output power is smaller by a factor of $\pi^2/16$ (-2.1 dB) than the maximum power obtained at saturation.

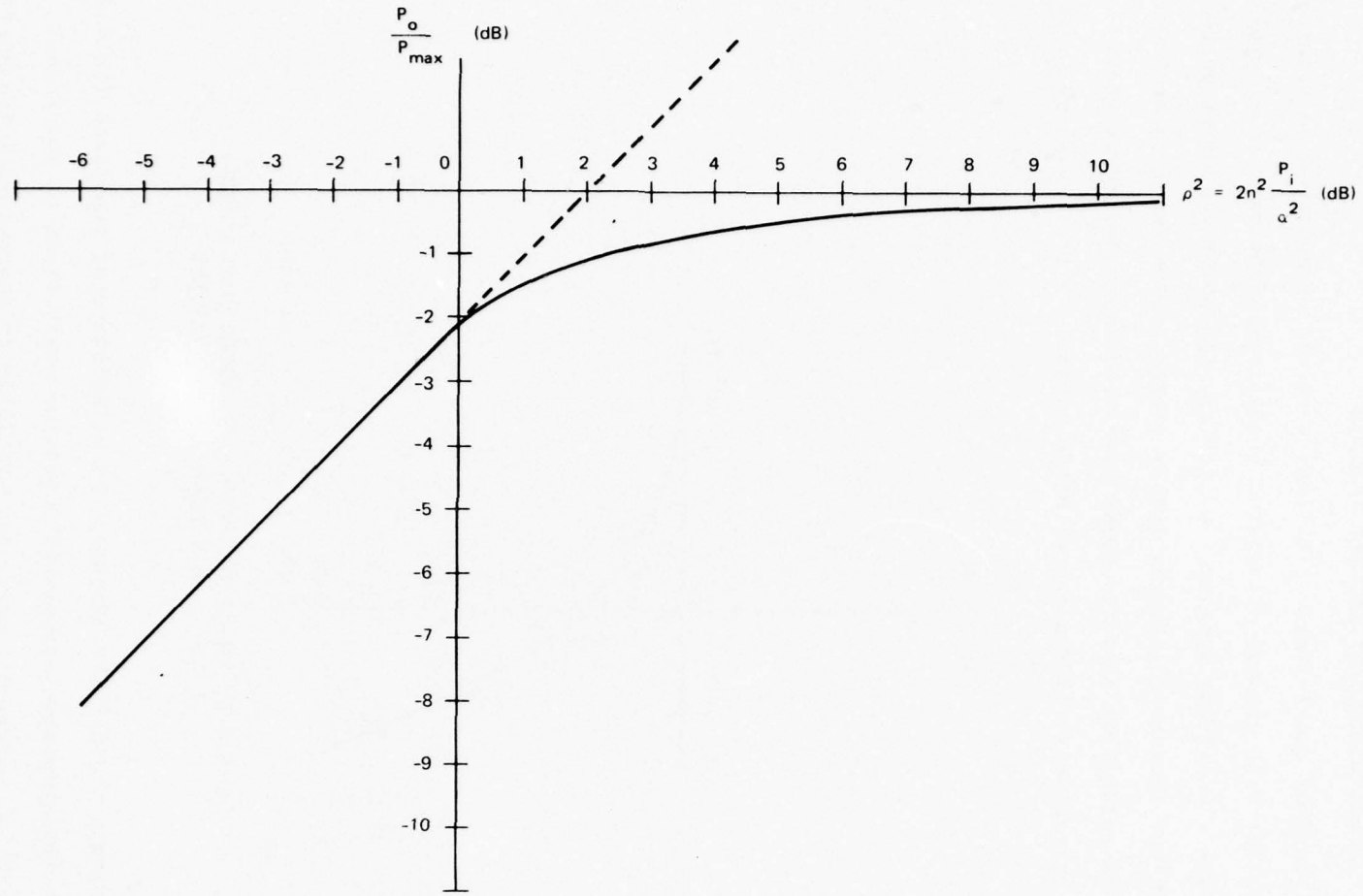

FIGURE A-6 NORMALIZED POWER OUTPUT OF A QUASI-LINEAR LIMITER

d. Practical Limiter Characteristics

Hard or quasi-linear limiting is rarely encountered in practice. A soft limiter with gradual saturation intuitively appears to most closely characterize a practical limiter. Generally, the power output of practical limiters increases linearly (unity slope) at low input power levels and reaches saturation at large power levels. Figure A-7 shows the measured characteristic of a tunnel diode limiter.[5] It is apparent that,

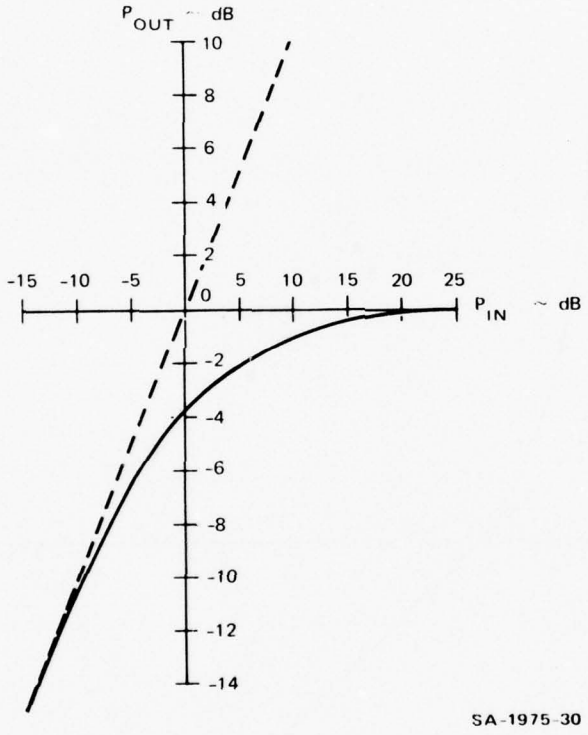

FIGURE A-7 MEASURED POWER TRANSFER CHARACTERISTIC OF A TUNNEL-DIODE LIMITER

to approximate closely the transfer characteristics of practical limiters, the analytical representation should provide unity slope at low signal levels, with an additional parameter available to characterize the softness with which the limiter reaches saturation.

The slope of the generalized limiter characteristic of Eq. (A-1) is:

$$\frac{dy}{dx} = \frac{2}{\pi} n \int_0^\infty \cos(vx) \cdot \sin(v\alpha/n)\, e^{-v^2\gamma^2/2}\, \frac{dv}{v} \quad .$$

Integration of the expression yields:

$$\frac{dy}{dx} = \frac{n}{2} \operatorname{erf}\left(\frac{\frac{\alpha}{n} + x}{\sqrt{2}\gamma}\right) + \frac{n}{2} \operatorname{erf}\left(\frac{\frac{\alpha}{n} - x}{\sqrt{2}\gamma}\right) \quad ; \qquad \text{(A-27)}$$

at low signal levels ($x \to o$),

$$\frac{dy}{dx} = n \operatorname{erf}\left(\frac{\alpha}{\sqrt{2}n\gamma}\right) \quad . \qquad \text{(A-28)}$$

The limiting level α is a fixed parameter determined by the specified power output when saturation is reached. From Eq. (A-20), it is

$$\alpha^2 = \frac{\pi^2}{8} P_{max} \quad . \qquad \text{(A-29)}$$

Requiring unity slope at low signals yields

$$n \operatorname{erf}\left(\frac{\alpha}{\sqrt{2}n\gamma}\right) = 1 \quad . \qquad \text{(A-30)}$$

Since the error function can never exceed one, n must be one or greater. Consider the two limiting cases for n. If $\gamma = 0$, n must be equal to one, since $\operatorname{erf}(\infty) = 1$. This represents the transfer characteristic of a quasi-linear limiter with unity slope. Figure A-8 shows the output/input power characteristic of a quasi-linear limiter with unity slope ($n = 1$) at low power levels. The limiting level α is chosen to provide 0-dB output power at saturation. If $n \to \infty$, the argument of the error function will tend to zero. Expanding the error function in a power series and

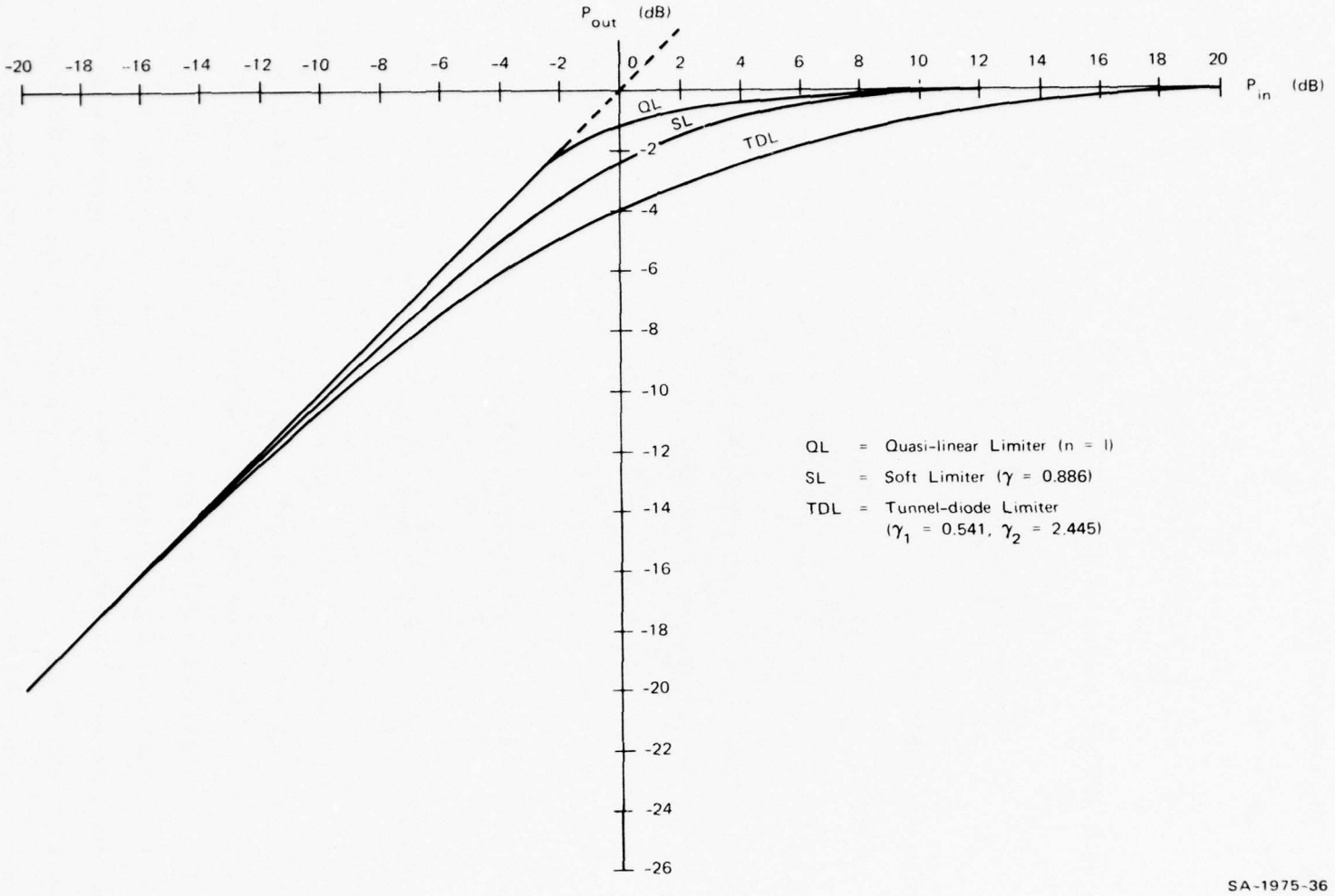

FIGURE A-8 POWER TRANSFER CHARACTERISTICS OF QUASI-LINEAR, SOFT, AND TUNNEL-DIODE LIMITERS

retaining only the first term yields:

$$\gamma = \sqrt{\frac{2}{\pi}}\,\alpha \quad . \tag{A-31}$$

Equation (A-31) is the relationship for determining γ for a soft limiter, if unity slope is required at low signal levels. Figure A-8 also shows the output/input power characteristic of a soft limiter with unity slope at low input power levels.

The first two curves in Figure A-8 correspond to the limiting values of n (1 and ∞). For all intermediate values of n, γ can be determined from Eq. (A-30). The curves representing the output/input power characteristic can be obtained from Eq. (A-12); they will all lie between these two curves.

Comparison of the soft-limiter curve in Figure A-8 with the curve in Figure A-7 shows that the tunnel diode limiter has a very soft saturation characteristic which cannot be approximated by Eq. (A-1). At 0-dB input power level, the output power of the tunnel diode limiter is approximately -4.0 dB, while a soft limiter having an error-function characteristic yields -2.2 dB.

Thus, if the limiting is very soft, representation of the limiter characteristic in terms of one error function [Eq. (A-4)] is not sufficient. Investigation showed, however, that the use of two additive error functions results in sufficient flexibility to describe even very soft limiter characteristics. The limiter characteristic is expressed as:

$$y = \frac{\alpha}{2}\left[\operatorname{erf}\left(\frac{x}{\sqrt{2}\gamma_1}\right) + \operatorname{erf}\left(\frac{x}{\sqrt{2}\gamma_2}\right)\right] \quad . \tag{A-32}$$

The parameters γ_1 and γ_2 can be appropriately chosen to approximate the measured characteristic closely. To determine γ_1 and γ_2, we need two independent equations. These can be obtained as follows. For small values of x, differentiation of Eq. (A-32) yields:

$$\frac{dy}{dx} = \frac{\alpha}{\sqrt{2\pi}} \left(\frac{1}{\gamma_1} + \frac{1}{\gamma_2} \right) \quad , \quad \text{for } x \to 0 \quad . \tag{A-33}$$

Requiring unity slope at low signal levels provides the first condition:

$$\frac{1}{\gamma_1} + \frac{1}{\gamma_2} = \frac{\sqrt{2\pi}}{\alpha} \quad . \tag{A-34}$$

A second equation is obtained by first specifying an output power for a given input power. For a sinusoidal input $x = a \cos \omega t$, the output is

$$g(t) = \frac{\alpha}{\sqrt{\pi}} \left[\rho_1 \cdot {}_1F_1\left(\frac{1}{2},\ 2,\ -\rho_1^2\right) + \rho_2 \cdot {}_1F_1\left(\frac{1}{2},\ 2,\ -\rho_2^2\right) \right] \cos \omega t \quad , \tag{A-35}$$

where

$$\rho_1^2 = \frac{a^2}{2\gamma_1^2} = \frac{P_i}{\gamma_1^2} \quad , \quad \rho_2^2 = \frac{a^2}{2\gamma_2^2} = \frac{P_i}{\gamma_2^2} \quad . \tag{A-36}$$

Equation (A-35) is obtained by summing the output of two error functions; the output of one error function is given by Eq. (A-14). The output power is then:

$$P_o = \frac{\alpha^2}{2\pi} \left[\rho_1 \cdot {}_1F_1\left(\frac{1}{2},\ 2,\ -\rho_1^2\right) + \rho_2 \cdot {}_1F_1\left(\frac{1}{2},\ 2,\ -\rho_2^2\right) \right]^2 \quad . \tag{A-37}$$

Specification of an output power P_{o1} at an input power P_{io} yields the second required equation:

$$\frac{1}{\gamma_1} \cdot {}_1F_1\left(\frac{1}{2},\ 2,\ -\frac{P_{io}}{\gamma_1^2}\right) + \frac{1}{\gamma_2} \cdot {}_1F_1\left(\frac{1}{2},\ 2,\ -\frac{P_{io}}{\gamma_2^2}\right) = \frac{\sqrt{2\pi}}{\alpha} \cdot \sqrt{\frac{P_{o1}}{P_{io}}} \quad . \quad \text{(A-38)}$$

Now, γ_1 and γ_2 can be determined by solving Eqs. (A-34) and (A-38). Explicit expressions for γ_1 and γ_2 are not possible because of the confluent hypergeometric functions involved in Eq. (A-38). However, they can be determined numerically by solving the two equations on a computer.

The curve labeled TDL (tunnel diode limiter) in Figure A-8 shows the power transfer characteristic based on Eq. (A-37). The parameters γ_1 and γ_2 were determined by specifying an output power level of -4.0 dB at 0-dB input power level, as shown by the measured TDL characteristic in Figure A-7. Comparison of the TDL curves in Figures A-7 and A-8 shows excellent agreement between the measured and theoretical results.

e. Summary

The voltage transfer characteristics of a quasi-linear, a soft, and a hard limiter can be expressed analytically in terms of infinite integrals by relating the limiter output to its input as summarized in Table A-1. In the case of soft limiting, the integral representation can also be expressed in terms of an error function. The power transfer characteristics of these limiter types are also shown in Table A-1.

In practice, the power output of limiters generally increases linearly with unity slope at low input power levels and reaches saturation at high power levels. The use of a quasi-linear or a soft limiter is restricted to producing a maximum of -2.2-dB power back-off at 0-dB input power consistent with unity slope at small input power levels and 0-dB output power at saturation. To achieve sufficient flexibility to describe limiters with substantial back-off--e.g., more than -2.2 dB at 0-dB input power--a slightly different representation is used for the limiter characteristic. The characteristic of such limiters can be

Table A-1

ANALYTICAL REPRESENTATION OF LIMITER CHARACTERISTICS

Limiter Type	Voltage Characteristic	Power Characteristic
Quasi-linear	$y = \frac{2}{\pi} n \int_0^\infty \sin(vx) \cdot \sin(v\alpha/n) \frac{dv}{v^2}$	$\frac{P_o}{P_{max}} = \frac{1}{4}\left[\sqrt{1 - \frac{1}{\rho^2}} + \rho \arcsin\left(\frac{1}{\rho}\right)\right]^2$, $\rho \geq 1$ $P_o = n^2 P_i$, $\rho \leq 1$; $\rho = 2n^2 P_i/\alpha^2$
Soft	$y = \frac{2\alpha}{\pi} \int_0^\infty \sin(vx)\, e^{-v^2\gamma^2/2} \frac{dv}{v}$ $= \alpha\, \mathrm{erf}(x/\sqrt{2}\gamma)$	$\frac{P_o}{P_{max}} = \frac{\pi}{4} \rho^2 \cdot {}_1F_1\left(\frac{1}{2}, 2, -\rho^2\right)$ $\rho^2 = P_i/\gamma^2$
Hard	$y = \frac{2\alpha}{\pi} \int_0^\infty \sin(vx) \frac{dv}{v}$	$\frac{P_o}{P_{max}} = 1$
Practical (very soft limiting)	$y = \frac{\alpha}{2}\left[\mathrm{erf}\left(\frac{x}{\sqrt{2}\gamma_1}\right) + \mathrm{erf}\left(\frac{x}{\sqrt{2}\gamma_2}\right)\right]$	$\frac{P_o}{P_{max}} = \frac{\pi}{16}\left[\rho_1 \cdot {}_1F_1\left(\frac{1}{2}, 2, -\rho_1^2\right) + \rho_2 \cdot {}_1F_1\left(\frac{1}{2}, 2, -\rho_2^2\right)\right]^2$ $\rho_1^2 = P_i/\gamma_1^2$, $\rho_2^2 = P_i/\gamma_2^2$

α = Limiting level (Figure A-2).

P_o = Limiter output power level.

n = Parameter to characterize the slope of the quasi-linear limiter (Figure A-3).

P_i = Limiter input power level (power in a single sinusoid).

P_{max} = Limiter output power level in saturation.

γ = Parameter to characterize the slope of the soft limiter (Figure A-4).

represented by the sum of two soft limiters each having an error-function characteristic as shown in Table A-1.

3. Bandpass Limiter Analysis

a. General

The most commonly used approach for determining the limiter output components, generally known as the characteristic function method, involves computing the autocorrelation function of the limiter output and then taking the Fourier transform to obtain the power density spectrum.[6] Although a general expression for the limiter output autocorrelation function can be derived, its computation becomes extremely involved when modulation of the input signals is considered. The difficulty lies in determining the characteristic function of the signals with arbitrary modulation. However, if the signals are statistically independent, angle-modulated sinusoids, and only the average power or the magnitude of the signal and cross-product terms at the limiter output is of interest, the modulation of the input signals can be ignored, which considerably simplifies the analysis. Davenport[6] was first to use this approach to investigate the effect of hard limiting a single unmodulated sinusoidal signal and narrow-band Gaussian noise. Jones[7] used the same method to analyze the case of two sinusoids plus noise. More recently, Shaft[8] and Gyi[9] independently extended the analyses to include n sinusoids.

The autocorrelation function method has the inherent drawback that the phase information of the signals and intermodulation components is lost when the autocorrelation function of the limiter output is determined. This approach is therefore not convenient for FDMA analysis, since the phases of the limiter output components are also of interest. For example, in the computation of the signal-to-intermodulation-power ratio for a given channel, the phases of the intermodulation components

falling in that channel are required, since the spreading of the power spectral density of any one cross-product term is a function of its phase modulation, even though the average power in that output component is independent of its phase. Another serious disadvantage of using the autocorrelation approach is that, since it yields only the autocorrelation function of the limiter output, the amplitude distribution of the interference (up-link noise and cross products) cannot be determined. To determine the bit-error probability in the detection of digitally phase-modulated signals, it is important to know the distribution of the noise and cross-product terms at the limiter output.

Stanford Research Institute has recently developed a time-domain method of analysis[20] that differs markedly from the older mathematical techniques widely used in the analysis of limiters. The main feature of this analytical approach is that it permits the limiter output--consisting of signals, intermodulation products, and noise--to be expressed completely in the time domain. Representation in the time domain permits retention of the phase of the FDMA signals and intermodulation products at the limiter output. The time-domain technique also permits evaluation of the distribution of the interfering signals (cross products and noise) at the limiter output. We use this analysis approach for determining the bandpass limiter output components and their distribution.

b. Calculation of the Limiter Output

The specific model for the bandpass limiter to be considered has been shown in Figure A-1. The input to the limiter,

$$x(t) = s(t) + n(t) \quad , \tag{A-39}$$

consists of the signal s(t) and a band of zero-mean stationary Gaussian noise n(t). It is assumed that the bandpass filter preceding the limiter

is wide enough to pass the signal with negligible distortion and limits the input noise to a narrow bandwidth that is small compared to the center frequency of the filter. The limiter is followed by another bandpass filter that confines the output spectrum essentially only to the fundamental band of the signal.

It is assumed that the limiter has a soft-limiting characteristic, described by an error-function relationship. Thus, if the limiter input is x(t), the output y(t) may be expressed in analytical form by Eq. (A-3) as

$$y(t) = \frac{2}{\pi} \alpha \int_0^\infty \sin[vx(t)]\, e^{-v^2\gamma^2/2}\, \frac{dv}{v} \quad . \tag{A-40}$$

The limiting level α is related to the maximum power output of the repeater by Eq. (A-20)

$$\alpha = \frac{\pi}{\sqrt{8}} \cdot \sqrt{P_{max}} \quad . \tag{A-41}$$

Here we analyze the problem with a soft limiter; the same approach, however, is applicable to the other limiter characteristics considered in Section 2. We therefore provide the required expressions for the signal, intermodulation, and noise components at the output of the bandpass limiter for the other limiter characteristics without derivation. When Expression (A-39) is inserted into Eq. (A-40), the sine of a sum may be expanded into the sum of two products of sine and cosine; thus,

$$y(t) = \frac{2}{\pi} \alpha \int_0^\infty \sin[vs(t)]\, \cos[vn(t)]\, e^{-v^2\gamma^2/2}\, \frac{dv}{v}$$

$$+ \frac{2}{\pi} \alpha \int_0^\infty \cos[vs(t)]\, \sin[vn(t)]\, e^{-v^2\gamma^2/2}\, \frac{dv}{v} \quad . \tag{A-42}$$

The narrow-band Gaussian noise at the limiter input may be expressed as

$$n(t) = r \cos\left(\omega_o t + \varphi\right) \quad , \tag{A-43}$$

where the envelope r and the phase φ are slowly time-varying random variables having Rayleigh and uniform distributions, respectively.

Substituting the above expression for the noise in Eq. (A-42) and using the general relationships

$$\sin(z \cos p) = 2 \sum_{m=o}^{\infty} (-1)^m J_{2m+1}(z) \cos(2m + 1)\, p$$

$$\cos(z \cos p) = J_o(z) + 2 \sum_{m=1}^{\infty} (-1)^m J_{2m}(z) \cos 2mp \quad , \tag{A-44}$$

the following expression for the limiter output is obtained:

$$y(t) = \frac{2}{\pi} \alpha \int_o^{\infty} \sin[v\, s(t)] \cdot J_o(vr)\, e^{-v^2\gamma^2/2} \frac{dv}{v}$$

$$+ \frac{4}{\pi} \alpha \sum_{m=1}^{\infty} (-1)^m \int_o^{\infty} \sin[v\, s(t)] \cdot J_{2m}(vr)\, e^{-v^2\gamma^2/2} \frac{dv}{v} \cos 2m\left(\omega_o t + \varphi\right)$$

$$+ \frac{4}{\pi} \alpha \sum_{m=o}^{\infty} (-1)^m \int_o^{\infty} \cos[v\, s(t)] \cdot J_{2m+1}(vr)\, e^{-v^2\gamma^2/2} \frac{dv}{v} \cos(2m + 1)\left(\omega_o t + \varphi\right) \quad . \tag{A-45}$$

All the terms in the above equation are random functions because of the presence of the noise envelope r and the phase φ. However, only the first integral will yield an average output, while the two other integrals will not contribute, since all the terms contain the random phase of the noise.

The average limiter output at any arbitrary time t is obtained by averaging over all possible noise amplitudes:

$$z(t) = E[y(t)] = \frac{2}{\pi} \alpha \int_0^\infty \sin[v\, s(t)] \cdot E\left[J_o(vr)\right] e^{-v^2\gamma^2/2} \frac{dv}{v} \quad . \quad \text{(A-46)}$$

Since the noise envelope has a Rayleigh distribution

$$p(r) = \frac{r}{\sigma^2} \exp\left(-\frac{r^2}{2\sigma^2}\right) \quad , \quad \text{(A-47)}$$

where σ^2 is the total noise power at the limiter input, the expected value of $J_o(vr)$ is given by

$$E\left[J_o(vr)\right] = \int_0^\infty J_o(vr)p(r)\, dr = \exp\left(-\frac{v^2\sigma^2}{2}\right) \quad . \quad \text{(A-48)}$$

Substitution of Eq. (A-48) in Eq. (A-46) yields

$$z(t) = \frac{2}{\pi} \alpha \int_0^\infty \sin[v\, s(t)] \cdot \exp\left[-\frac{v^2\left(\sigma^2 + \gamma^2\right)}{2}\right] \frac{dv}{v} \quad . \quad \text{(A-49)}$$

The above integral may also be written in terms of the error function[1] as:

$$z(t) = \alpha\, \mathrm{erf}\left[\frac{s(t)}{\sqrt{2\left(\sigma^2 + \gamma^2\right)}}\right] \quad . \quad \text{(A-50)}$$

The corresponding expressions for the case of a hard limiter are obtained by setting $\gamma = 0$ in Eqs. (A-49) and (A-50). The presence of noise at the input of a soft limiter thus tends to make the limiting even softer,

because of the gradual saturation characteristics of the error function. This was also observed by Jones.[7] The effect of soft limiting on the average output is mathematically identical to adding noise to a hard limiter, provided that an error-function representation can be used for the soft-limiter characteristic.

The components that collectively make up the limiter output noise spectrum are the second and third integrals of Eq. (A-45):

$$\eta(t) = \frac{4}{\pi}\,\alpha \sum_{m=1}^{\infty} (-1)^m \int_0^{\infty} \sin[v\ s(t)]\ J_{2m}(vr)\ e^{-v^2\gamma^2/2}\ \frac{dv}{v} \cos\ 2m\left(\omega_o t + \varphi\right)$$

$$+ \frac{4}{\pi}\,\alpha \sum_{m=o}^{\infty} (-1)^m \int_0^{\infty} \cos[v\ s(t)]\ J_{2m+1}(vr)\ e^{-v^2\gamma^2/2}\ \frac{dv}{v} \cos(2m+1)\left(\omega_o t + \varphi\right) \quad . \qquad \text{(A-51)}$$

Expressions (A-49) and (A-51) are the two fundamental equations for the analysis of the limiter in the time domain. In Davenport's notation,[6] Eq. (A-49) represents the output signal and intermodulation components resulting from the interaction of the signal with itself (s × s terms). Similarly, Eq. (A-51) represents output noise components that are due to the interaction of the input noise with itself (n × n terms) and with the input signal (s × n terms). Separation of the noise output into n × n terms and s × n terms is not possible, without knowledge of the signal waveform s(t).

If the characteristic function method had been used to calculate the limiter output, the phases of all the components at the limiter output would have been lost, and a separation of the output components as in Eqs. (A-49) and (A-51) would have been possible only in terms of the autocorrelation function of the individual components.

c. Limiting of n Signals and Noise

1) General

The signal and intermodulation products at the limiter output are obtained by inserting the expression for the limiter input signals

$$s(t) = \sum_{i=1}^{n} a_i \cos\left[\omega_i t + \Phi_i(t)\right] \quad , \tag{A-52}$$

where a_i and $\Phi_i(t)$ represent the amplitude and phase modulation of the FDMA carriers, into Eq. (A-49), and using the general relationship:

$$\sin\left(\sum_{i=1}^{n} \beta_i \cos \alpha_i\right) = \sum_{p_1=-\infty}^{\infty} \cdots \sum_{p_n=-\infty}^{\infty} \left\{\prod_{i=1}^{n} J_{p_i}(\beta_i) \sin\left[\sum_{i=1}^{n} p_i\left(\alpha_i + \frac{\pi}{2}\right)\right]\right\} \quad , \tag{A-53}$$

where the symbol $\prod$ indicates that all n of the J_{p_i} coefficients are multiplied together. Thus, the limiter output, prior to bandpass filtering, is given by

$$z(t) = \frac{1}{2} \sum_{p_1=-\infty}^{\infty} \cdots \sum_{p_n=-\infty}^{\infty} h_{p_1 p_2 \cdots p_n} \sin\left\{\sum_{i=1}^{n} p_i\left[\omega_i t + \Phi_i(t) + \frac{\pi}{2}\right]\right\} \quad , \tag{A-54}$$

where

$$h_{p_1 p_2 \cdots p_n} = \frac{4}{\pi} \alpha \int_0^{\infty} \prod_{i=1}^{n} J_{p_i}(v a_i) \exp\left[-\frac{v^2\left(\sigma^2 + \nu^2\right)}{2}\right] \frac{dv}{v} \tag{A-55}$$

represents the amplitude coefficient of the output signal and intermodulation components.

Note that the modulation of the signals affects only the phase of the intermodulation components, as can be seen from Eq. (A-54), and that the amplitudes of the signals and intermodulation components [Eq. (A-55)] are independent of modulation. Equation (A-55) is dependent

only on the characteristic of the limiter and the amplitudes of the signals at the limiter input. Such a separation between the amplitude and phase of the limiter output components is extremely convenient, particularly for the analysis and computation of the intermodulation components. The significance of the parameters in Eq. (A-55) is as follows:

- n is the total number of signals (accesses).
- The value of p_i is the harmonic of the i^{th} signal appearing in the cross product under consideration. Thus, $p_i = 0$ indicates that the i^{th} signal does not contribute to the cross product, while $p_i = 1$ indicates that the fundamental appears, and so forth. The composition of the cross product is indicated by the subscript $p_1 p_2 \ldots p_n$. A subscript 100...0 indicates that the output term under consideration is Signal 1. A subscript 2100...0 indicates that the second harmonic of Signal 1 is mixed with the fundamental of Signal 2, and so forth.
- a_i is the amplitude (voltage) of the i^{th} input signal.
- σ^2 is the noise power at the input to the limiter. Thus, $a_i^2/2\sigma^2$ is the SNR of the i^{th} signal at the input to the limiter.

2) Amplitude of Limiter Output Components

The limiter output, given by Eq. (A-54), was derived by assuming soft limiting. In the case of hard-limiting and quasi-linear-limiting characteristics (Figure A-3), only Eq. (A-55) will be modified.

The expression for the case of a hard limiter is obtained by setting $\gamma = 0$ in Eq. (A-55). For the case of a quasi-linear limiter with unity slope ($n = 1$ and $\gamma = 0$), the following expression for the amplitude coefficients is obtained:

$$h_{p_1 p_2 \cdots p_n} = \frac{4}{\pi} \int_0^\infty \prod_{i=1}^{n} J_{p_i}(va_i) \sin(v\alpha) \exp\left(-\frac{v^2\sigma^2}{2}\right) \frac{dv}{v^2} \quad . \quad \text{(A-56)}$$

When the limiting is very soft, the limiter characteristic can be described by a sum of two soft limiters, represented by error-function characteristics with different slope parameters. Thus, if the limiter characteristic is represented by Eq. (A-32), the limiter output, prior to bandpass filtering, will be given by Eq. (A-54). The amplitude coefficient in this case is equal to the sum of the amplitude coefficients of two error functions of slope parameters γ_1 and γ_2, respectively,

$$h_{p_1 p_2 \cdots p_n} = \frac{2}{\pi} \alpha \int_0^\infty \prod_{i=1}^{n} J_{p_i}(va_i) \left\{ \exp\left[-\frac{v^2\left(\sigma^2 + \gamma_1^2\right)}{2}\right] + \exp\left[-\frac{v^2\left(\sigma^2 + \gamma_2^2\right)}{2}\right] \right\} \frac{dv}{v} \quad . \quad \text{(A-57)}$$

A closed-form solution for the amplitudes of the output components is extremely difficult for n larger than three. For n equal to three or less, the amplitudes of the signals and intermodulation components can be obtained in terms of hypergeometric functions by using the expressions derived in Ref. 10. A much more straightforward approach that is valid for all values of n would be to determine the amplitudes by numerically evaluating the integral of Eqs. (A-55) and (A-56). A computer program for evaluating Eqs. (A-55) and (A-57) is discussed in Appendix C. This program can easily be extended to compute Eq. (A-56) by including the additional sine term.

3) Frequency and Phase of Limiter Output Components

Equation (A-54) shows that the limiter output will contain components whose frequency and phase are given by:

$$f = p_1 f_1 + p_2 f_2 + \ldots + p_n f_n$$

$$\Phi(t) = p_1 \Phi_1(t) + p_2 \Phi_2(t) + \ldots + p_n \Phi_n(t) + \frac{\pi}{2}\left(p_1 + p_2 + \ldots + p_n\right) \quad , \quad \text{(A-58)}$$

where

$$p_1, p_2, \ldots, p_n = (0, \pm 1, \pm 2, \ldots).$$

Obviously, these relationships will remain the same whether hard or soft limiting is used; in fact, they hold for all odd-power devices. We make the following definitions:

- The zone of an intermodulation product is the sum of the p_i coefficients:

$$\text{Zone} = p_1 + p_2 + \ldots + p_n \quad . \qquad \text{(A-59)}$$

- The order of an intermodulation product is the sum of the magnitudes of the p_i coefficients:

$$\text{Order} = |p_1| + |p_2| + \ldots + |p_n| \quad . \qquad \text{(A-60)}$$

Here, we are interested only in the terms that fall in the first zone,

$$p_1 + p_2 + \ldots + p_n = 1 \quad , \qquad \text{(A-61)}$$

since all other terms will be filtered out by the bandpass filter following the limiter.

It is apparent that the determination of all the terms that will fall in the pass band of the filter is quite a formidable task when n is large. Fortunately, Shaft[2] has shown that the dominant output components are the signal and cross-product terms for which $|p_i|_{max}$ is small (≤ 2). This approximation considerably simplifies Eq. (A-54), since, instead of considering all the p_i from $-\infty$ to ∞, it is necessary to consider them only in the range from -2 to 2. The significant filter output components may be determined by first considering the different frequency combinations in Eq. (A-54) and then selecting the desired ones, i.e., the combinations that will yield frequencies in the pass band.

Since the limiter has an odd-order transfer characteristic, only the third- and fifth-order intermodulation components are the significant contributors to the output distortion. As can be seen from Eq. (A-60), for the third-order intermodulation products, the sum of the magnitudes of the p_i coefficients is three, while for the fifth-order cross products it is five. The frequencies of the third- and fifth-order cross products are shown in Table A-2.

4) Determination of Limiter Output Noise Components

The components that collectively make up the soft-limiter output noise may be obtained by substituting Eq. (A-52) for s(t) in Eq. (A-51), and expanding sin[v s(t)] and cos[v s(t)] with the aid of Eq. (A-53). The expansion of cos [v s(t)] will contain cosine terms instead of the sine in Eq. (A-53). The resulting expression then represents the combined output noise produced because of the interaction of the input noise with itself (n × n terms) and that produced as a result of the interaction of the input signal with noise (s × n terms). In this

Table A-2

FREQUENCIES OF THIRD- AND FIFTH-ORDER CROSS PRODUCTS

Order	Frequency
3	$f_a + f_b - f_c = f_{111}$
3	$2f_a - f_b = f_{21}$
5	$f_a + f_b + f_c - f_d - f_e = f_{11111}$
5	$2f_a + f_b - f_c - f_d = f_{2111}$
5	$f_a + f_b + f_c - 2f_d = f_{1112}$
5	$2f_a + f_b - 2f_c = f_{212}$
5	$3f_a - f_b - f_c = f_{311}$
5	$3f_a - 2f_b = f_{32}$

expression, the term corresponding to m and all p_i equal to zero represents the direct feedthrough noise (n × n terms), and all the remaining terms constitute the noise produced by the mixing of the signal with the limiter input noise (s × n terms). The expression for the direct feedthrough noise (n × n terms) is given by

$$\eta_{n\times n}(t) = \frac{4}{\pi}\,\alpha \int_0^\infty J_1(vr) \prod_{i=1}^{n} J_o\left(va_i\right) e^{-v^2\gamma^2/2}\,\frac{dv}{v}\left[\cos\,\omega_o t + \varphi(t)\right] \quad . \quad \text{(A-62)}$$

Davenport[6] has shown, for the case of one signal and noise, that only the n × n terms contribute significantly to the output noise at low limiter input SNRs. When the number of signals is sufficiently large that the amplitude distribution of their sum is approximately Gaussian, the SNR for any one signal will be small at the limiter input. Consequently, from Davenport's results, it is reasonable to expect that only the direct feedthrough noise will contribute significantly to the limiter output noise.

By using an exponential approximation for the product of the Bessel functions

$$\prod_{i=1}^{n} J_o\left(va_i\right) \approx \exp\left(-\frac{1}{2} v^2 \sigma_2^2\right) \quad , \tag{A-63}$$

where

$$\sigma_2^2 = \sum_{i=1}^{n} \frac{a_i^2}{2} \tag{A-64}$$

represents the total power of all the input signals, Eq. (A-62) can be readily integrated to yield:

$$\eta_{n\times n}(t) = \alpha \sqrt{\frac{2}{\pi}}\left[\frac{r(t)}{\sigma_3}\right] {}_1F_1\left[\frac{1}{2}, 2, -\frac{r^2(t)}{2\sigma_3^2}\right] \cos\left[\omega_o t + \varphi(t)\right] \quad , \tag{A-65}$$

where $\sigma_3^2 = \gamma^2 + \sigma_2^2$.

In FDMA, the total power in all the input signals is much larger than the power in the up-link noise at the limiter input. The confluent hypergeometric function in Eq. (A-65) may be set equal to unity to a very good approximation. This can be shown by calculating the expectation of the hypergeometric function:

$$E\left\{{}_1F_1\left[\frac{1}{2},\ 2,\ -\frac{r^2(t)}{2\sigma_3^2}\right]\right\} = \frac{\Gamma(2)}{\Gamma(1/2)}\sum_{n=o}^{\infty}\frac{(-1)^n\cdot\Gamma\left(n+\frac{1}{2}\right)}{\Gamma(n+2)\cdot n!}E\left[\frac{r^2(t)}{2\sigma_3^2}\right]^n$$

$$= \frac{\Gamma(2)}{\Gamma(1/2)}\sum_{n=o}^{\infty}\frac{(-1)^n\cdot\Gamma\left(n+\frac{1}{2}\right)}{\Gamma(n+2)}\left(\frac{\sigma}{\sigma_3}\right)^{2n} \quad , \qquad \text{(A-66)}$$

since

$$E\left[r^{2n}(t)\right] = \int_o^{\infty} r^{2n}p(r)\,dr = n!\cdot\left(2\sigma^2\right)^n \quad , \qquad \text{(A-67)}$$

where $p(r)$ is given by a Rayleigh distribution [Eq. (A-47)], and σ^2 is the total noise power at the limiter input. Because in FDMA σ/σ_3 is very much less than one, the series in Eq. (A-66) can be approximated by the first term, yielding a value of unity for the expectation of the confluent hypergeometric function. With this approximation, Eq. (A-65) simplifies to:

$$\eta_{n\times n}(t) = \sqrt{\frac{2}{\pi}}\left(\frac{\alpha}{\sigma_3}\right)r(t)\cos\left[\omega_o t + \varphi(t)\right] \quad . \qquad \text{(A-68)}$$

Equation (A-68) shows that the bandpass limiter output noise will tend to have a Gaussian distribution of variance

$$\sigma_n^2 = \frac{2}{\pi}\left(\frac{\alpha}{\sigma_3}\right)^2\sigma^2 \quad . \qquad \text{(A-69)}$$

It can be seen that Eq. (A-68) represents the dominant output noise in the time domain. This representation is particularly useful for the evaluation of the system following the bandpass limiter. Equation (A-68) may also be represented in the form

$$\eta_{n\times n}(t) = x_1(t)\cos\omega_o t - y_1(t)\sin\omega_o t \quad , \qquad \text{(A-70)}$$

where $x_1(t)$ and $y_1(t)$, the amplitudes of the "in-phase" and "quadrature" components, are given by:

$$x_1(t) = \sqrt{\frac{2}{\pi}} \left(\frac{\alpha}{\sigma_3}\right) r(t) \cos \varphi(t) \qquad \text{(A-71)}$$

$$y_1(t) = \sqrt{\frac{2}{\pi}} \left(\frac{\alpha}{\sigma_3}\right) r(t) \sin \varphi(t) \quad . \qquad \text{(A-72)}$$

The functions $x_1(t)$ and $y_1(t)$ are Gaussian random variables having zero mean and equal variance given by Eq. (A-69).

Expressions (A-68) through (A-72) are also applicable for a hard limiter ($\gamma = 0$). The only change will be to replace σ_3^2 in these expressions by σ_2^2. If the limiting is very soft, so that the limiter characteristic is described by the sum of two soft limiters represented by error-function characteristics with different slope parameters, the bandpass limiter output noise can be obtained by summing the noise contribution of the two soft limiters. Analogously to Eq. (A-68) we obtain in this case:

$$\eta_{n\times n}(t) = \sqrt{\frac{2}{\pi}} \left[\left(\frac{\alpha}{2\sigma_4}\right) + \left(\frac{\alpha}{2\sigma_5}\right)\right] r(t) \cos\left[\omega_o t + \varphi(t)\right] \quad , \qquad \text{(A-73)}$$

where

$$\sigma_4^2 = \sigma_2^2 + \gamma_1^2 \quad , \qquad \sigma_5^2 = \sigma_2^2 + \gamma_2^2 \quad . \qquad \text{(A-74)}$$

Here σ_2^2 is the total power in all the input signals, while γ_1 and γ_2 are the slope parameters of the two soft limiters.

d. Summary

Using a time-domain analysis approach, general expressions for the amplitude, frequency, and phase of the signals and intermodulation products at the output of the bandpass limiter have been obtained for the case when the limiter input consists of n phase-modulated carriers of arbitrary amplitudes and noise. The amplitudes of the signals and cross products can be determined by numerical evaluation of an infinite integral for the different limiter characteristics considered in Section 2. Equations have also been obtained to determine the frequency and phase of the limiter output components. It has also been possible to obtain the distribution of the up-link noise at the bandpass limiter output. Since, in FDMA, the total signal power at the repeater input is much larger than the noise power, the distribution of the noise at the repeater output may be considered Gaussian.

4. Conclusions

Analytical expressions for the nonlinear transfer characteristic of a quasi-linear, a soft, and a hard limiter can be obtained from an infinite integral representation that relates the limiter output to its input. In the case of a soft limiter, the integral expression is identical to an error-function representation commonly used to characterize a soft limiter. Generally, the power output of practical limiters increases linearly (unity slope) at low input power levels and reaches saturation at large power levels. Representation of the limiter transfer characteristics as a sum of two soft limiters each represented by an error function ensures unity slope at low signal levels, with an additional parameter available to characterize the softness with which the limiter reaches saturation.

The effect of ideal bandpass limiting on an arbitrary signal lying in narrow-band, stationary, zero-mean Gaussian noise has been analyzed, and general analytic expressions for the limiter output components have been derived by using a time-domain approach. A major advantage of the time-domain method is that it preserves the phases of the signal and intermodulation products, which are destroyed in the characteristic function method generally used in limiter studies. Expressions for the desired signal and intermodulation product amplitudes have been obtained for the case when the input consists of n phase-modulated signals of arbitrary amplitudes and noise. The amplitudes of the signals and intermodulation components can be determined by numerically evaluating an infinite integral for the different limiter characteristics. It has also been possible to obtain a time-domain representation for the limiter output noise, which is particularly useful for the evaluation of the system following the bandpass limiter. If the total signal power at the limiter input is much greater than the repeater noise power, the distribution of the noise at the repeater output can be considered Gaussian.

Appendix B

ERROR-RATE INVESTIGATION

Appendix B

ERROR-RATE INVESTIGATION

1. General

The objective of this appendix is to provide a comprehensive analysis of the problem of detection of n quadriphase-modulated, constant-envelope PSK/FDMA carriers after transmission through a wideband limiting satellite transponder. Specifically, the goal of the study is to develop the expression for the bit-error rate at the output of an FDMA channel, taking into consideration the presence of (1) other FDMA carriers causing adjacent-channel interference, (2) cross products generated as a result of the mixing of the FDMA signals in the limiting repeater, and (3) retransmitted up-link (satellite repeater) as well as down-link (receiver) noise.

2. Quadriphase Detection

A digital quadriphase-modulated carrier can be expressed as:

$$s(t) = A \cos\left[\omega_i t + \Phi_i(t) + \theta_i\right] \quad , \qquad \text{(B-1)}$$

where ω_i is the carrier radian frequency, and θ_i is a constant phase angle. The phase modulation $\Phi_i(t)$ at any instant can take one of four values: $\pi/4$, $3\pi/4$, $5\pi/4$, or $7\pi/4$. By expanding the cosine, it can easily be seen that the quadriphase signal can also be expressed as the sum of two orthogonal biphase-modulated signals (each having half the data rate of the quadriphase modulation),

$$s(t) = \frac{A}{\sqrt{2}} \left[\cos \Phi_i(t) \cos\left(\omega_i t + \theta_i\right) - \sin \Phi_i(t) \sin\left(\omega_i t + \theta_i\right)\right]$$

$$= \frac{A}{\sqrt{2}} \left[u_i(t) \cos\left(\omega_i t + \theta_i\right) - v_i(t) \sin\left(\omega_i t + \theta_i\right)\right] \quad , \quad \text{(B-2)}$$

where $u_i(t)$ and $v_i(t)$ are two independent binary (± 1) waveforms of equal data rate. Figure B-1 depicts the principle for generating a quadriphase signal based on Eq. (B-2).

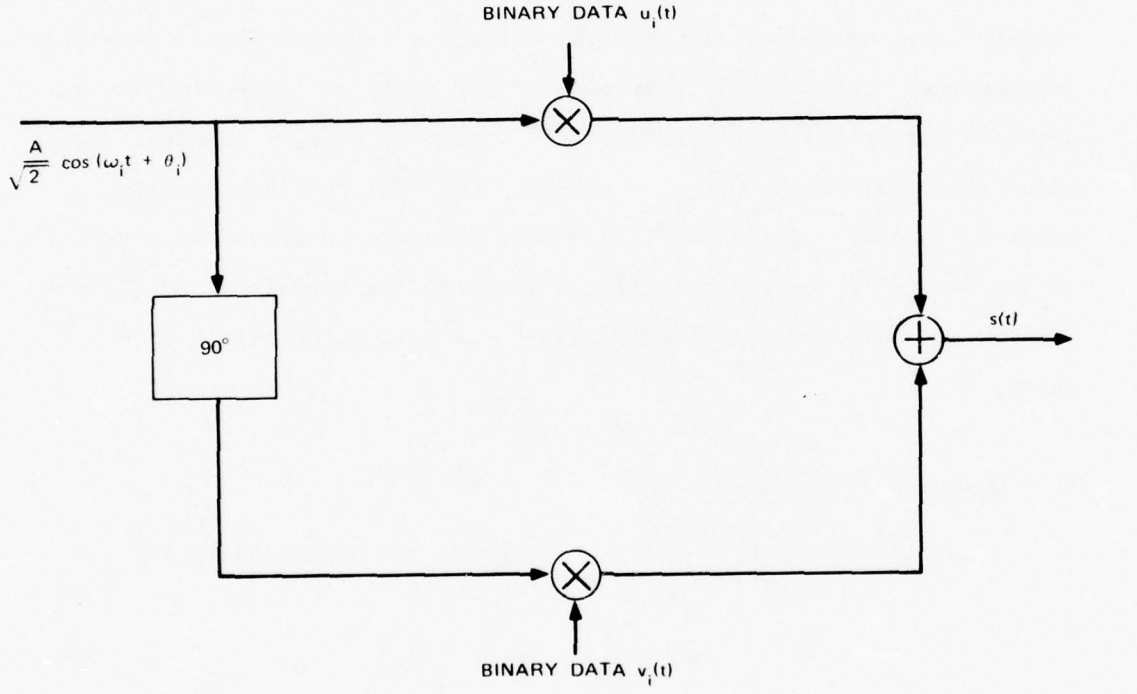

FIGURE B-1 PRINCIPLE FOR GENERATING A QUADRIPHASE SIGNAL

The scheme for detecting a quadriphase-modulated carrier is shown in Figure B-2. It represents the receiving scheme for the detection of two orthogonal biphase-modulated carriers. The upper channel of Figure B-2 detects the data modulation $u_i(t)$, and the lower channel detects

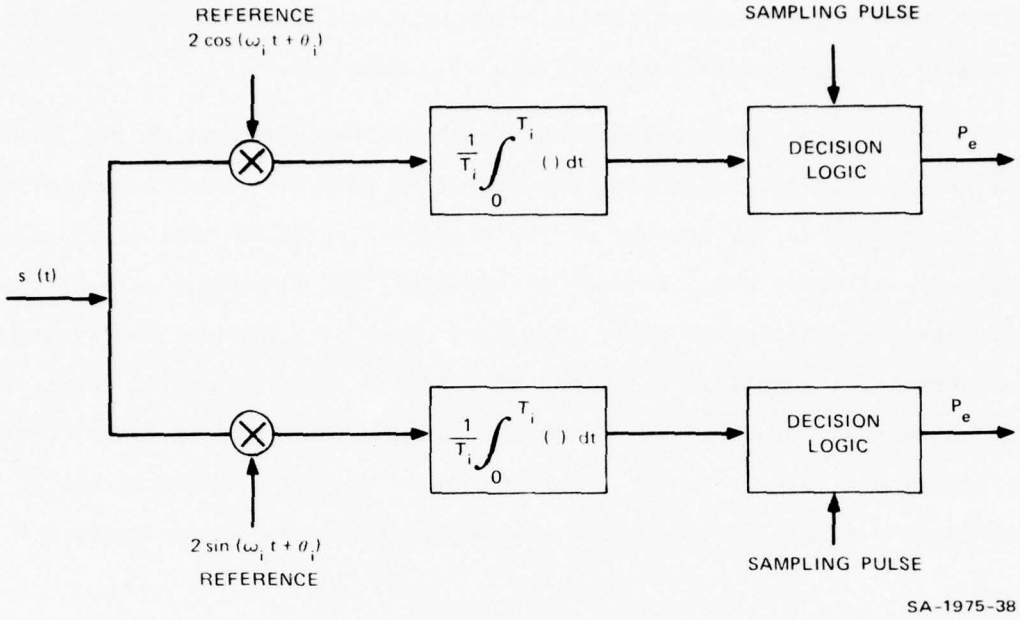

FIGURE B-2 CORRELATION RECEIVER FOR DETECTION OF A QUADRIPHASE SIGNAL

$v_i(t)$. No interference occurs between the two channels, because the two sinusoidal carriers are in quadrature and therefore are orthogonal.

3. Approach for Determining the Error Rate

For determining the error rate of any FDMA channel, it will be assumed that all the transmitters in the system employ quadriphase modulation of the FDMA carriers and that the corresponding receivers use the detection scheme shown in Figure B-2. In practice, a wideband RF bandpass filter will usually precede the detector in Figure B-2. The purpose of this filter is to ease the problem of initial receiver synchronization by removing out-of-band signals and intermodulation products without appreciably distorting the desired signal. For the evaluation of the error rate, we may assume that receiver synchronization has been achieved and consequently the RF filter is not required. The suppression of the

out-of-band signals and intermodulation products is accomplished by the low-pass (integrate-and-dump) filters of Figure B-2.

Since a quadriphase-modulated signal can be expressed as two orthogonal biphase-modulated signals, the bit-error rate of a quadriphase system can be defined as the average of the bit-error rates of the two biphase channels in Figure B-2. Because of symmetry, the bit-error rate of the two channels will be the same. The error rate of a quadriphase system is, therefore, identical with that of a biphase system, and it suffices to consider the probability of error of either the upper or lower channel in Figure B-2 only. For the error analysis, the FDMA receivers can be represented simply as single biphase detectors, as shown in Figure B-3.

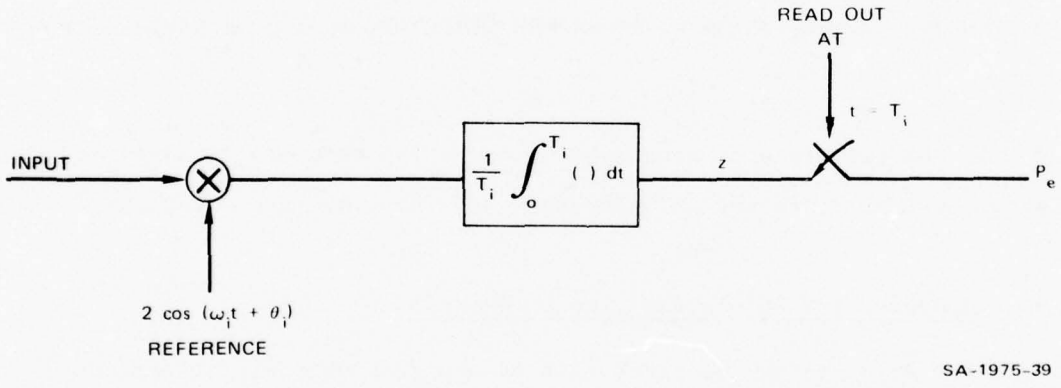

FIGURE B-3 RECEIVER MODEL FOR ERROR-RATE CALCULATION

At the receiver output in Figure B-3, the decision whether a mark or a space has been transmitted is made on the basis of whether the filter output at the sampling instant is positive or negative. If it is assumed that the transmission of a mark or a space signal is equally probable and that the noise at the filter output has a zero-mean value, then the probability of error, P_e, in a decision is equal to the error

probability in either a mark or a space signal. The probability of error in detecting a mark is equal to the probability that the filter output will be negative at the sampling instant. Thus, P_e is given by

$$P_e = \int_{-\infty}^{o} p(z)\, dz \quad , \tag{B-3}$$

where p(z) is the probability density function of the filter output. To calculate P_e, one needs to determine p(z), which may be obtained by first calculating the characteristic function of the filter output and then taking the Fourier transform:

$$p(z) = \frac{1}{2\pi} \int_{-\infty}^{\infty} C_z(\xi)\, e^{-i\xi z}\, d\xi \quad , \tag{B-4}$$

where $C_z(\xi)$ is the characteristic function of the random variable z at the output.

In nonlinear systems, such as in the case of FDMA where the signals and up-link noise have passed before detection through a limiter having a nonlinear characteristic, this transform poses a formidable problem, since the expression for the characteristic function is usually extremely complex. Alternatively, it is much more convenient to calculate the error probability directly from the characteristic function. It can be shown that, if z is any random variable of probability density function p(z) and characteristic function $C_z(\xi)$, its cumulative distribution function, P(a), is given by:[11]

$$P(a) = \int_{-\infty}^{a} p(z)\, dz = \frac{1}{2} - \frac{1}{\pi} \int_{o}^{\infty} I_m\left[C_z(\xi) \cdot e^{-i\xi a}\right] \frac{d\xi}{\xi} \quad , \tag{B-5}$$

where I_m denotes that only the imaginary part has to be taken. Comparison of Eqs. (B-3) and (B-5) shows that

$$P_e = P(0) = \frac{1}{2} - \frac{1}{\pi} \int_0^\infty I_m\left[C_z(\xi)\right] \frac{d\xi}{\xi} \quad . \qquad \text{(B-6)}$$

Thus, the approach for calculating P_e for any FDMA channel will be to determine $C_z(\xi)$ at the channel output for a mark transmission and then to perform the integration in Eq. (B-6). It should be noted that Eq. (B-6) is a general result that can be used to determine P_e for a linear as well as a nonlinear channel of arbitrary transfer characteristic.

4. Determination of $C_z(\xi)$

To derive the mathematical expression for $C_z(\xi)$ at the receiver output in Figure B-3, it will be necessary first to obtain the expression for the receiver output z at the sampling instant. To achieve this we write an expression for the signals and noise components present at the receiver input and then develop the expression for the output.

Appendix A shows that when the input to the satellite repeater consists of n constant-envelope quadriphase-modulated FDMA carriers and up-link noise, the repeater output will contain, in addition to the signals and noise components, intermodulation products resulting from the mixing of the signals in the limiter. All these components will also be present at each receiver input, but their amplitudes will be modified because of the power loss on the down-link transmission and the amplification in the receiver front end. In addition to these signals, received from the satellite, down-link noise will be present at the input to the receiver.

Thus, in an FDMA system the input to the i^{th} receiver will comprise the components considered below.

The Desired Signal Component

$$s_i(t) = a_i \left[\cos \omega_i t + \Phi_i(t) + \theta_i\right]$$

$$= \frac{a_i}{\sqrt{2}} \left[u_i(t) \cos\left(\omega_i t + \theta_i\right) - v_i(t) \sin\left(\omega_i t + \theta_i\right)\right] \quad , \quad \text{(B-7)}$$

where $u_i(t)$ and $v_i(t)$ are independent binary (± 1) data modulation of the orthogonal carriers, and θ_i is a random phase angle.

The Undesired Signal Components

$$s_k(t) = \sum_{\substack{k=1 \\ k \neq i}}^{n} a_k \cos\left[\omega_k t + \Phi_k(t) + \theta_k\right] \quad , \quad \text{(B-8)}$$

where $\Phi_k(t)$ represents quadriphase modulation of the signals, and θ_k is the random phase of the carriers.

The Intermodulation Components

$$I(t) = \sum_{j=1}^{m} b_j \cos\left[\omega_j t + \psi_j(t) + \alpha_j\right] \quad , \quad \text{(B-9)}$$

where $\psi_j(t)$ represents the phase modulation of the intermodulation products; α_j is the random phase angle; and m is the number of cross products falling in the repeater bandwidth.

Expressions for determining the amplitudes, phases, and frequencies of the signals and intermodulation products at the output of the satellite repeater are given in Appendix A. The expressions for the signal amplitude and the intermodulation products at the receiver input can be obtained from their corresponding expressions at the satellite repeater output by taking into consideration the losses on the down link and the gain in the receiver. The frequencies and phases of the intermodulation products in Eq. (B-9) are dependent, respectively, on the frequencies and phases of the signals. The number of intermodulation products falling

in the repeater bandwidth m is solely a function of the number of FDMA signals at the repeater input and their frequencies. For the calculation of the error rate we assume a frequency assignment for the signals, so the number of in-hand intermodulation products m, their frequencies ω_j, and their phases $\psi_j(t)$, α_j can be determined from the knowledge of the frequencies and phases of the signals producing these cross products.

The Noise Components

The receiver input noise consists of the sum of the retransmitted up-link noise and the Gaussian down-link or receiver front-end noise. Appendix A shows that the distribution of the up-link noise at the repeater output will be to a good approximation Gaussian, since the total FDMA signal power at the repeater input is much larger than the up-link noise power. Thus the distribution of the retransmitted up-link noise at the receiver input will also be Gaussian; only its variance relative to that at the repeater output will be different. This can be determined by taking into account the down-link losses and the amplification in the receiver. Since both the up-link and the down-link noise at the receiver input are independent and zero-mean Gaussian, the composite noise will also be Gaussian with zero mean and variance equal to the sum of the variances.

The input to the i^{th} receiver in Figure B-3 can be expressed as

$$r(t) = \frac{a_i}{\sqrt{2}} \left[u_i(t) \cos\left(\omega_i t + \theta_i\right) - v_i(t) \sin\left(\omega_i t + \theta_i\right)\right] + n(t)$$
$$+ \sum_k a_k \cos\left[\omega_k t + \Phi_k(t) + \theta_k\right]$$
$$+ \sum_j b_j \cos\left[\omega_j t + \psi_j(t) + \alpha_j\right] \quad . \qquad \text{(B-10)}$$

Here, n(t) denotes the composite receiver input Gaussian noise (sum of retransmitted up-link and down-link noise).

The receiver output z in Figure B-3 is obtained by cross correlating the input r(t) with the synchronized receiver reference $2\cos[\omega_i t + \theta_i]$ over the bit interval T_i of the desired signal,

$$z = \frac{1}{T_i} \int_0^{T_i} r(t) \cdot 2 \cos\left(\omega_i t + \theta_i\right) dt \quad . \tag{B-11}$$

(Note T_i is equal to $2/R_i$, where R_i is the bit rate of the quadriphase signal.) Substituting Eq. (B-10) into Eq. (B-11) and assuming that a mark was transmitted $[u_i(t) = 1]$, the output is given by:

$$z = \frac{a_i}{\sqrt{2}} + \eta$$

$$+ \sum_k a_k \cdot \frac{1}{T_i} \int_0^{T_i} \cos\left[\left(\omega_k - \omega_i\right)t + \phi_k(t) + \theta_k - \theta_i\right] dt$$

$$+ \sum_j b_j \cdot \frac{1}{T_i} \int_0^{T_i} \cos\left[\left(\omega_j - \omega_i\right)t + \psi_j(t) + \alpha_j - \theta_i\right] dt \quad . \tag{B-12}$$

The carrier with modulation $v_i(t)$ in Eq. (B-10) will not produce any output, since it is orthogonal to the receiver reference. The parameter η in Eq. (B-12) denotes the receiver output noise. Since the receiver input noise n(t) is assumed to be Gaussian and the receiving system is linear, the distribution of the output noise η will also be Gaussian with zero mean and variance given by:

$$\sigma_i^2 = \int_{-\infty}^{\infty} |H(f)|^2 \cdot G(f)\, df \quad . \tag{B-13}$$

where G(f) is the spectral density of the receiver input noise, and H(f) is the transfer function of the integrate-and-dump filter in Figure B-3.

By expanding the cosines in Eq. (B-12) and rearranging the output, z can be written as:

$$z = \frac{a_i}{\sqrt{2}} + \eta + \sum_k A_{ik} \cos \theta_{ik} + \sum_j B_{ij} \cos \alpha_{ij} \quad , \qquad \text{(B-14)}$$

where the amplitudes and phases of the undesired signals and intermodulation products at the receiver output are defined as:

$$A_{ik} = a_k \cdot \sqrt{\beta_{ik}^2 + \gamma_{ik}^2}$$

$$B_{ij} = b_j \cdot \sqrt{\hat{\beta}_{ij}^2 + \hat{\gamma}_{ij}^2} \qquad \text{(B-15)}$$

$$\theta_{ik} = \theta_k - \theta_i + \arctan \gamma_{ik}/\beta_{ik}$$

$$\alpha_{ij} = \alpha_j - \theta_i + \arctan \hat{\gamma}_{ij}/\beta_{ij} \quad . \qquad \text{(B-16)}$$

The quantities β and γ in Eqs. (B-15) and (B-16) represent the effect of filtering on the signals and cross products. They are given by:

$$\beta_{ik} = \frac{1}{T_i} \int_o^{T_i} \cos\left[\left(\omega_k - \omega_i\right)t + \phi_k(t)\right] \, dt \qquad \text{(B-17a)}$$

$$\gamma_{ik} = \frac{1}{T_i} \int_o^{T_i} \sin\left[\left(\omega_k - \omega_i\right)t + \phi_k(t)\right] \, dt \qquad \text{(B-17b)}$$

$$\hat{\beta}_{ij} = \frac{1}{T_i} \int_o^{T_i} \cos\left[\left(\omega_j - \omega_i\right)t + \psi_j(t)\right] \, dt \qquad \text{(B-17c)}$$

$$\hat{\gamma}_{ij} = \frac{1}{T_i} \int_o^{T_i} \sin\left[\left(\omega_j - \omega_i\right)t + \psi_j(t)\right] \, dt \quad . \qquad \text{(B-17d)}$$

The β_{ik} and γ_{ik}, as well as $\hat{\beta}_{ij}$ and $\hat{\gamma}_{ij}$, are random variables, because they are dependent on the random modulation $\phi_k(t)$ of the FDMA carriers. It should be remembered that the phase modulation $\psi_j(t)$ of the cross products is a function of the modulation $\phi(t)$ of the signals.

Equation (B-14) represents the output of the receiver when its input consists of signals, cross products, and noise. To calculate the error probability by Eq. (B-6), we need the characteristic function $C_z(\xi)$ of the receiver output z. The first two terms in Eq. (B-14) represent the sum of the desired signal and the contribution of the receiver input noise at the output. The last two terms containing the summations represent the contributions of the undesired signals and the intermodulation products. Since the first two terms are statistically independent of the last two, $C_z(\xi)$ can be expressed as the product of the characteristic function of the signal plus noise and the characteristic function of the sum of the undesired signals and the cross products:

$$C_z(\xi) = e^{i\xi a_i/\sqrt{2}} \cdot e^{-\sigma_i^2 \xi^2/2} \cdot C(\xi) \quad . \qquad \text{(B-18)}$$

Here, $C(\xi)$ denotes the characteristic function of the sum of the undesired signals and the intermodulation components in Eq. (B-14).

The angles θ_{ik} and α_{ij} in Eq. (B-14) are uniformly distributed and are also statistically independent. The amplitude A_{ik} of any one undesired signal at the i^{th} receiver output is dependent only on the random modulation $\phi_k(t)$ of that signal. But the amplitude B_{ij} of any given

cross product is dependent on the phase modulations of the signals that generate that cross product. Averaging first over the distributions of θ_{ik} and α_{ij} gives:

$$C(\xi) = E\left[\prod_k J_o\left(A_{ik} \cdot \xi\right) \cdot \prod_j J_o\left(B_{ij} \cdot \xi\right)\right] \quad , \qquad \text{(B-19)}$$

where E[ ] denotes the expectation of A_{ik} and B_{ij} with respect to the random phase modulation Φ_k of the signals. Substitution of Eq. (B-19) into Eq. (B-18) yields:

$$C_z(\xi) = e^{i\xi a_i/\sqrt{2}} \cdot e^{-\sigma_i^2 \xi^2/2} \cdot E\left[\prod_k J_o\left(A_{ik} \cdot \xi\right) \cdot \prod_j J_o\left(B_{ij} \cdot \xi\right)\right] \quad . \qquad \text{(B-20)}$$

In the special case when the FDMA signals are unmodulated [$\Phi_k(t) = 0$], all A_{ij} and B_{ij} will be constants and we would not need to evaluate the expectation in Eq. (B-20).

In the derivation of Eq. (B-20), it is implicitly assumed that the amplitudes of the signals and cross products (a_i, a_k, b_j) at the receiver input are constants. Strictly, because of the presence of up-link noise at the limiter input, these amplitudes will be random variables dependent only on the amplitude distribution (Rayleigh distribution) of the up-link noise. Thus, Eq. (B-20) should also be averaged over the amplitude distribution of the up-link noise. Since, in FDMA, the total signal power at the limiter input is much larger than the input noise power, the fluctuation in the amplitudes of signals and cross products caused by the presence of noise will be small and can be neglected without producing significant error in the determination of $C_z(\xi)$. Thus, instead of averaging Eq. (B-20) we assume that the amplitudes a_i, a_k, and a_j are the expected values (averaged over the amplitude distribution of the input noise). They are then identical with the h parameters discussed

in Appendix A, with the parameter α modified to take into account the gains and losses from the limiter output to the receiver input. This approximation includes in the analysis the suppression and power-sharing effects of the up-link noise and neglects the slight fluctuation caused by noise in the amplitudes of signals and cross products at the limiter output.

5. Determination of P_e

Substitution of the imaginary part of Eq. (B-20) in Eq. (B-6) yields the following expression for the bit-error probability at the output of the i^{th} channel:

$$P_{ei} = \frac{1}{2} - \frac{1}{\pi} \int_o^\infty \frac{\sin\left(\xi a_i/\sqrt{2}\right)}{\xi} \cdot E\left[\prod_k J_o\left(A_{ik} \cdot \xi\right) \cdot \prod_j J_o\left(B_{ij} \cdot \xi\right)\right] \cdot e^{-\sigma_i^2 \xi^2/2} \, d\xi \quad . \quad \text{(B-21)}$$

It can be seen that in Eq. (B-21) the $\sin \xi/\xi$ term is a maximum at $\xi = 0$ and decreases rapidly as ξ increases. The same is true for the exponential term. The value of $J_o(\ )$ is unity for $\xi = 0$ and less than unity for all other values of ξ. As the number of terms in the product increases, the value of the product becomes small, except when all terms are near unity, i.e., when ξ is near zero. Since the integrand of Eq. (B-21) is the product of the three terms, which decrease with increasing ξ, the major contribution to the integral will stem from the values of these terms near $\xi = 0$. In the neighborhood of $\xi = 0$, we can expand the Bessel functions in a power series and use the following approximations:

$$E\left[\prod_k J_o\left(A_{ik} \cdot \xi\right) \cdot \prod_j J_o\left(B_{ij} \cdot \xi\right)\right] = 1 - \frac{\xi^2}{2} E\left[\sum_k \frac{A_{ik}^2}{2} + \sum_j \frac{B_{ij}^2}{2}\right]$$

$$+ \text{terms in } \xi^4 \text{ and higher}$$

$$\approx 1 - \frac{\xi^2}{2}\left[\sum_k P_{ik} + \sum_j \hat{P}_{ij}\right] \qquad \text{(B-22)}$$

$$\approx e^{-\xi^2/2}\left[\sum_k P_{ik} + \sum_j \hat{P}_{ij}\right] , \qquad \text{(B-23)}$$

where

$$P_{ik} = \frac{1}{2} E\left[A_{ik}^2\right] = \frac{a_k^2}{2} E\left[\beta_{ik}^2 + \gamma_{ik}^2\right]$$

$$\hat{P}_{ij} = \frac{1}{2} E\left[B_{ij}^2\right] = \frac{b_j^2}{2} E\left[\hat{\beta}_{ij}^2 + \hat{\gamma}_{ij}^2\right] \qquad \text{(B-24)}$$

are respectively the average signal and cross-product powers at the receiver output. The summations in Eq. (B-22) represent the total power contribution of all the undesired signals and the intermodulation products at the output of the i^{th} receiver.

The left-hand side of Eq. (B-22) represents the product of the characteristic functions of independent sinusoids. If the number of sinusoids is large, the resultant characteristic function can be approximated by the characteristic function of Gaussian noise [Eq. (B-23)], which is justified by the central limit theorem. For as few as four signals, we have in Eq. (B-22) a product of 27 Bessel functions (three signals, 24 third-order cross products). For ten signals, the number of Bessel functions increases to 459. So it can be seen that the approximation of Eq. (B-23) will improve as the number of signals increases.

Using the approximation of Eq. (B-22) in Eq. (B-21) and evaluating the integral yields:

$$P_{ei} = \frac{1}{2}\left[1 - \operatorname{erf}\left(\rho_i/\sqrt{2}\right)\right] + \frac{\rho_i}{2\sigma_i^2}\left[\sum_k P_{ik} + \sum_j \hat{P}_{ij}\right]\frac{e^{-\rho_i^2/2}}{\sqrt{2\pi}} \quad , \qquad \text{(B-25)}$$

where $\rho_i^2 = a^2/2\sigma_i^2$. On the other hand, substituting Eq. (B-23) into Eq. (B-21) and performing the integration gives:

$$P_{ei} = \frac{1}{2}\left[1 - \operatorname{erf}\left(r_i/\sqrt{2}\right)\right] \quad , \qquad \text{(B-26)}$$

where

$$r_i^2 = \frac{a_i^2/2\sigma_i^2}{1 + \sum_k P_{ik}/\sigma_i^2 + \sum_j \hat{P}_{ij}/\sigma_i^2} \qquad \text{(B-27)}$$

represents the equivalent SNR at the output of the i^{th} channel.

It can be seen from the numerical tables that for small x the value of $J_o(x)$ lies between

$$1 - \frac{x^2}{4} < J_o(x) < e^{-x^2/4} \quad .$$

Thus, the approximation of Eq. (B-22) will yield a lower bound on the error probability [Eq. (B-25)], while the exponential approximation will give the upper bound [Eq. (B-26)]. The true probability of error will lie between these two values. As the number of signals n increases, the number of third-order cross products increases as $n^2(n - 1)/2$, and the total number of Bessel functions involved in Eq. (B-21) increases as $(n - 1) + n^2(n - 1)/2$. Thus, from the central limit theorem, it is reasonable to expect the true error rate to be closer to the upper bound given by Eq. (B-26). We therefore use this upper bound to determine the error rate at the output of the i^{th} FDMA channel.

The output SNR of Eq. (B-27) can also be expressed as

$$r_i^2 = \frac{\rho_i^2}{1 + \sum_{\substack{k=1 \\ k \neq i}}^{n} \rho_{ik}^2 S_{ik} + \sum_j \hat{\rho}_{ij}^2 \hat{S}_{ij}} \quad , \tag{B-28}$$

where

$\rho_i^2 = a_i/2\sigma_i^2$ = SNR for the desired signal

$\rho_{ik}^2 = a_k^2/2\sigma_i^2$ = SNR for the k^{th} signal

$\hat{\rho}_{ij}^2 = b_j^2/2\sigma_i^2$ = intermodulation-to-noise ratio for the j^{th} cross product

and

$$S_{ik} = E\left[\beta_{ik}^2 + \gamma_{ik}^2\right]$$

$$\hat{S}_{ij} = E\left[\hat{\beta}_{ij}^2 + \hat{\gamma}_{ij}^2\right] \quad . \tag{B-29}$$

The parameters S_{ik} and $\hat{S}_{ij}$ represent the effect of filtering in the i^{th} receiver on the k^{th} interfering link and on the j^{th} cross product, respectively.

The approximation of Eq. (B-23) amounts to modeling the composite distribution of the sum of all the undesired FDMA signals and the cross products as equivalent Gaussian noise at the output of the receiver. This approximation is not the same as assuming their distribution to be Gaussian at the receiver input. If care is not exercised, the latter approximation will lead to errors in the calculation of the variance of the Gaussian distribution at the receiver output. For example, consider the contributions of the two third-order cross products,

$$A \cos\left[\left(\omega_i + \omega_1 - \omega_2\right)t + \alpha_i + \alpha_1 - \alpha_2\right]$$

and

$$A \cos\left[\left(\omega_i + \omega_2 - \omega_1\right)t + \alpha_i + \alpha_2 - \alpha_1\right] \quad ,$$

to the receiver output. These are generated as a result of the mixing of the desired signal at the frequency f_i with two other signals at frequencies f_1 and f_2. If these cross products are considered independent at the receiver input (this is required by the Gaussian assumption), their contributions to the receiver output can be obtained by summing the power contribution of each, taking into account their power spectra and the transfer function of the integrate-and-dump filter.

However, more accurately, the contribution of these two cross products is obtained by cross correlation with the receiver reference. Multiplication of both the cross products with the receiver reference will yield a single baseband waveform, $2A \cos[(\omega_1 - \omega_2)t + \alpha_1 - \alpha_2]$, of twice the amplitude, because the two cross products add coherently in amplitude. The power contribution at the receiver output can then be obtained by integrating the power spectrum multiplied by the square of the magnitude of the transfer function of the filter. This more accurate procedure leads to a 3-dB-larger value for the output power contribution from these two cross products than the one obtained by considering them as independent sinusoids at the receiver input.

The time-domain approach takes into account any coherency between cross products at every stage of the receiver; it therefore provides an accurate determination of their contribution to the receiver output. The approximation of Eq. (B-23) is based on determining the contribution of all the undesired FDMA signals and cross products at the receiver output, taking into account their coherency, and then approximating them as Gaussian noise.

6. Determination of S_{ik} and $\hat{S}_{ii}$

Consider first the determination of S_{ik}:

$$S_{ik} = E\left(\beta_{ik}^2 + \gamma_{ik}^2\right) \quad ,$$

where

$$\beta_{ik} = \frac{1}{T_i} \int_o^{T_i} \cos\left[\Delta\omega_k t + \phi_k(t)\right] dt$$

$$\gamma_{ik} = \frac{1}{T_i} \int_o^{T_i} \sin\left[\Delta\omega_k t + \phi_k(t)\right] dt \qquad \text{(B-30)}$$

and

$$\Delta\omega_k = \omega_k - \omega_i \quad .$$

Here, the expectation has to be evaluated over the distribution of $\phi_k(t)$ during the bit interval $0 \leq t \leq T_i$.

From Eq. (B-30) it can be seen that the expectation of β_{ik}^2 will be the same as that of γ_{ik}^2. Thus, we can write

$$S_{ik} = 2 \cdot E\left(\beta_{ik}^2\right) \quad . \qquad \text{(B-31)}$$

The expectation of β_{ik}^2 can be calculated as follows:

$$E\left(\beta_{ik}^2\right) = \frac{1}{T_i^2}\int_o^{T_i}\int_o^{T_i} E\left\{\cos\left[\Delta\omega_k t_1 + \phi_k\left(t_1\right)\right] \cdot \cos\left[\Delta\omega_k t_2 + \phi_k\left(t_2\right)\right]\right\} dt_1 dt_2$$

$$= \frac{1}{2T_i^2}\int_o^{T_i}\int_o^{T_i} E\left\{\cos\left[\Delta\omega_k\left(t_2 - t_1\right) + \phi_k\left(t_2\right) - \phi_k\left(t_1\right)\right]\right\} dt_1 dt_2$$

$$= \frac{1}{T_i^2}\int_o^{T_i}\int_o^{T_i} R_{\phi_k}\left(t_2 - t_1\right)\cos\left[\Delta\omega_k\left(t_2 - t_1\right)\right] dt_1 dt_2 \quad , \qquad \text{(B-32)}$$

where $R_{\phi_k}(t_2 - t_1)$ represents the autocorrelation function of the quadriphase modulation $\phi_k(t)$. The last line of Eq. (B-32) is obtained by expanding the cosine in the previous line and using the relationships

$$R_{\phi_k}\left(t_2 - t_1\right) = E\left[\sin\,\phi_k\left(t_1\right) \cdot \sin\,\phi_k\left(t_2\right)\right] = E\left[\cos\,\phi_k\left(t_1\right) \cdot \cos\,\phi_k\left(t_2\right)\right]$$

and

$$E\left[\sin\,\phi_k\left(t_1\right) \cdot \cos\,\phi_k\left(t_2\right)\right] = E\left[\sin\,\phi_k\left(t_2\right) \cdot \cos\,\phi_k\left(t_1\right)\right] = 0 \quad . \qquad \text{(B-33)}$$

Defining the impulse response of the integrate and dump filter in Figure B-3 as:

$$h_i(t) = 1/T_i \qquad \text{for } 0 \le t \le T_i$$

$$= 0 \qquad t > T_i \quad ,$$

we can express Eq. (B-32) as:

$$E\left(\beta_{ik}^2\right) = \int_o^{\infty}\int_o^{\infty} R_{\phi_k}\left(t_2 - t_1\right)\cos\,\Delta\omega_k\left(t_2 - t_1\right) \cdot h_i\left(t_1\right) \cdot h_i\left(t_2\right) dt_1 dt_2 \quad . \qquad \text{(B-34)}$$

Replacing t_2 by $t_1 + \tau$ in the above expression yields:

$$E\left(\beta_{ik}^2\right) = \int_0^\infty \int_{-\infty}^\infty R_{\phi_k}(\tau) \cdot \cos \Delta\omega_k \tau \cdot h_i\left(t_1\right) \cdot h_i\left(t_1 + \tau\right) dt_1 d\tau \quad . \quad \text{(B-35)}$$

If the filter autocorrelation function is defined as

$$R_{h_i}(\tau) = \int_0^\infty h_i\left(t_1\right) \cdot h_i\left(t_1 + \tau\right) dt_1 \quad , \quad \text{(B-36)}$$

we obtain, finally, the relationship:

$$E\left(\beta_{ik}^2\right) = \int_{-\infty}^\infty R_{\phi_k}(\tau) \cdot R_{h_i}(\tau) \cdot \cos \Delta\omega_k \tau \, d\tau \quad . \quad \text{(B-37)}$$

Substituting Eq. (B-37) in Eq. (B-31), we obtain:

$$S_{ik} = 2 \int_{-\infty}^\infty R_{\phi_k}(\tau) \cdot R_{h_i}(\tau) \cdot \cos \Delta\omega_k \tau \, d\tau \quad . \quad \text{(B-38)}$$

It can be shown that the filter autocorrelation $R_{h_i}(\tau)$ is a triangle given by:

$$R_{h_i}(\tau) = \frac{1}{T_i}\left(1 - \frac{|\tau|}{T_i}\right) \quad , \quad \text{for } |\tau| \leq T_i \quad . \quad \text{(B-39)}$$

The autocorrelation function of the quadriphase signal modulation $R_{\phi_k}(\tau)$ can be determined as follows:

$$R_{\phi_k}(\tau) = E\left[\cos \phi_k(t) \cdot \cos \phi_k(t + \tau)\right]$$

$$= \frac{1}{2} E\left[u_k(t) \cdot u_k(t + \tau)\right]$$

$$= \frac{1}{2} R_{u_k}(\tau) \quad , \quad \text{(B-40)}$$

where $u_k(t)$ is a binary (± 1) random waveform whose autocorrelation function is represented by $R_{u_k}(\tau)$. Since the autocorrelation function of a binary random waveform is a triangle, $R_{u_k}(\tau)$ can be expressed as:

$$R_{u_k}(\tau) = \left(1 - \frac{|\tau|}{T_k}\right) \quad , \qquad \text{for } |\tau| \leq T_k \quad , \tag{B-41}$$

where $1/T_k$ is the bit rate of the biphase modulation. The parameter S_{ik} can now be evaluated with the aid of Eqs. (B-39) through (B-41).

Similarly, for $\hat{S}_{ij}$ we obtain the following expression analogous to Eq. (B-38):

$$\hat{S}_{ij} = 2 \int_{-\infty}^{\infty} R_{\psi_j}(\tau) \cdot R_{h_i}(\tau) \cos \Delta\omega_j \tau \, d\tau \quad , \tag{B-42}$$

where

$$\Delta\omega_j = \omega_j - \omega_i \quad ,$$

and $R_{\psi_j}(\tau)$ is the autocorrelation function of the phase modulation of the intermodulation product

$$R_{\psi_j}(\tau) = E\left[\cos \psi_j(t) \cdot \cos \psi_j(t + \tau)\right] \quad . \tag{B-43}$$

The evaluation of $R_{\psi_j}(\tau)$ is best described by an example. Suppose we want to determine the autocorrelation function of a third-order cross product having the phase modulation $\psi(t) = \Phi_1(t) + \Phi_2(t) - \Phi_3(t)$. This cross product is generated as a result of mixing three input signals in the limiter with the phase modulations $\Phi_1(t)$, $\Phi_2(t)$, and $\Phi_3(t)$, respectively. In terms of signal modulations, Eq. (B-43) can be expressed as:

$$R_{\psi_j}(\tau) = E\Big\{\cos\left[\phi_i(t) + \phi_2(t) - \phi_3(t)\right] \cdot \cos\left[\phi_1(t+\tau) + \phi_2(t+\tau) - \phi_3(t+\tau)\right]\Big\} \quad . \quad \text{(B-44)}$$

By expanding the cosines and using the statistical independence between the phase modulations of the signals, it can be shown that

$$R_{\psi_j}(\tau) = 4R_{\phi_1}(\tau) \cdot R_{\phi_2}(\tau) \cdot R_{\phi_3}(\tau) \quad , \quad \text{(B-45)}$$

where the $R_{\phi}(\tau)$'s are the autocorrelation functions of the random quadriphase modulation of the signals. Each $R_{\phi}(\tau)$ can be expressed in terms of a biphase autocorrelation function $R_u(\tau)$, as in Eq. (B-38). We thus obtain

$$R_{\psi_j}(\tau) = \frac{1}{2} R_{u_1}(\tau) \cdot R_{u_2}(\tau) \cdot R_{u_3}(\tau) \quad , \quad \text{(B-46)}$$

where each $R_u(\tau)$ is a triangle defined as:

$$R_{u_i}(\tau) = 1 - \frac{|\tau|}{T_i} \quad , \quad \text{for } |\tau| \leq T_i \quad , \quad i = 1,2,3 \quad . \quad \text{(B-47)}$$

Equation (B-42) can now be evaluated with the aid of Eqs. (B-46) and (B-47).

Using this approach, we can determine the power contribution of any desired intermodulation product at the receiver output. A special case, however, occurs in dealing with the cross products generated as a result of the mixing of the desired signal with other signals. For example, consider the case where we want to determine the power contribution of a third-order intermodulation product that has the modulation

$$\psi(t) = \phi_1(t) + \phi_2(t) - \phi_i(t) \quad ,$$

where $\Phi_i(t)$ is the phase modulation of the desired signal. Since the receiver will be synchronized with the desired signal, i.e., with $\Phi_i(t)$, the output power for this cross product will be independent of $\Phi_i(t)$ and will depend only on the random switching of $\Phi_1(t)$ and $\Phi_2(t)$ during the integration interval of the matched low-pass filter. The autocorrelation function $R_{\psi_j}(\tau)$ in this case will be determined by the autocorrelation functions of Φ_1 and Φ_2:

$$R_{\psi_j}(\tau) = E\left\{\cos\left[-\Phi_i(t) + \Phi_2(t)\right] \cdot \cos\left[\Phi_1(t+\tau) + \Phi_2(t+\tau)\right]\right\}$$

$$= 2\, R_{\Phi_1}(\tau) \cdot R_{\Phi_2}(\tau)$$

$$= \frac{1}{2} R_{u_1}(\tau) \cdot R_{u_2}(\tau) \quad . \tag{B-48}$$

Similar expressions can be derived for treating cross products of other orders that are generated by mixing of the desired signal with other signals in the limiter.

7. Summary

By using a time-domain analysis approach, a general expression [Eq. (B-21)] has been obtained for determining the bit-error probability in detecting a desired quadriphase-modulated FDMA signal at the receiver, when n independent FDMA signals are transmitted simultaneously through a limiting satellite transponder. The error-rate expression has been derived under the assumption that small fluctuations in the amplitudes of the signals and cross products caused by the random envelope of the limiter input noise can be ignored and that the distribution of the uplink noise at the output of the repeater can be considered Gaussian. In an FDMA system, these assumptions are permissible under the condition

that the total power in all the signals at the repeater input is much larger than the power in the up-link noise.

Exact evaluation of Eq. (B-21) is very difficult because of the problem involved in determining the expectations of the receiver output amplitudes of the interfering FDMA signals and the cross products caused by random modulation of the carriers. However, it has been possible to obtain the upper and lower bounds within which the error rate is expected to lie. When the number of FDMA signals is large, the error rate is expected to be close to the upper bound.

Appendix C

DESCRIPTION OF THE COMPUTER PROGRAM SYSCON

Appendix C

DESCRIPTION OF THE COMPUTER PROGRAM SYSCON

1. General

The computer program SYSCON has been developed to model an FDMA satellite communication system and to investigate and optimize its performance in operation with a mix of user terminals of differing characteristics, such as data rates, transmitter ERPs, and receiver sensitivities (G/T). The capability to improve system performance is achieved through optimization of a norm representing the figure of merit or a measure of the system's communication performance.

Two norms have been selected for optimization:

$$N_a = \sum_{i=1}^{n} P_{ei} \tag{C-1}$$

and

$$N_b = \sum_{i=1}^{n} P_{ei} \cdot R_i \Big/ \sum_{i=1}^{n} R_i \quad , \tag{C-2}$$

where

P_{ei} = error probability of the i^{th} channel

R_i = data rate of the i^{th} channel.

The norm N_a treats all links equally and does not take into consideration the fact that some links may carry information at higher data rates than others. This fact is taken into account in norm N_b, which represents the

sum of error probabilities weighted by the data rates. Either of these two norms can be selected for system optimization in SYSCON.

2. Model of the Satellite Repeater

The model of the satellite repeater used in SYSCON is shown in Figure C-1. It consists of a receiving antenna followed by a bandpass filter, a high-gain preamplifier, a limiter, a bandpass filter, a TWT amplifier, and finally, the transmitting antenna. Both the preamplifier and the TWT amplifier are assumed to be linear, so all the nonlinearity existing in the repeater can be attributed to the presence of the bandpass limiter sandwiched between the two amplifiers. Both the bandpass filters are assumed to be ideal. The input filter is wide enough to pass the signals with negligible distortion and limits the input noise to a bandwidth that is small compared to the frequencies of the signals. The bandpass filter following the limiter confines the limiter output spectrum essentially only to the fundamental band of the input signals. In practice, the repeater will also contain a frequency translator that ideally has no effect on the system performance. In SYSCON the up-link frequencies are shifted down by an amount Δf ($\Delta f = 0.725$ GHz) prior to transmission through the limiter. This shift translates the up-link signal frequencies to their correct values for down-link transmission.

3. Limiter Characteristic

The measured power input/output transfer characteristic of a tunnel-diode bandpass limiter is shown in Appendix A, Figure A-7. Both the input and the output power levels are normalized with respect to the maximum power output of the limiter P_{omax}. The dashed line in Figure A-7 shows the normalized power transfer characteristic of a linear amplifier of unity gain.

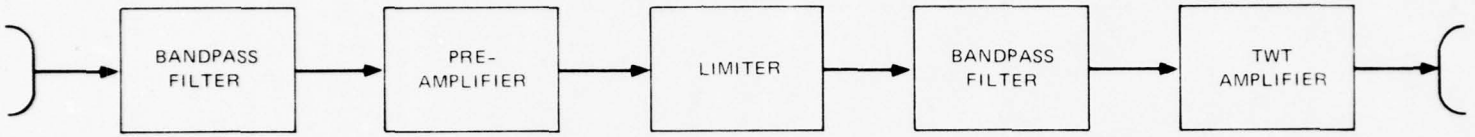

FIGURE C-1 MODEL OF THE SATELLITE REPEATER USED IN SYSCON

To approximate closely the transfer characteristics of practical limiters such as that shown in Figure A-7, the analytical representation must provide unity slope at low signal levels, with an additional parameter available to characterize the softness with which the limiter reaches saturation. This can be achieved by describing the limiter voltage characteristic by a sum of two error functions [Appendix A, Eq. (A-32)]:

$$y = \frac{\alpha}{2}\left[\operatorname{erf}\left(\frac{x}{\sqrt{2}\gamma_1}\right) + \operatorname{erf}\left(\frac{x}{\sqrt{2}\gamma_2}\right)\right] \quad , \tag{C-3}$$

where α is the limiting level. The parameters γ_1 and γ_2 can be chosen appropriately to approximate the measured power transfer characteristic (such as in Figure A-7) of practical limiters.

a. Normalization

It is convenient first to normalize the maximum output power of the limiter to 0 dBW for the determination of the two limiter parameters γ_{10} and γ_{20} (the subscript 0 refers to the values with respect to 0-dBW power output). The values of γ_1 and γ_2 can then be calculated for an arbitrary maximum limiter power output in terms of γ_{10} and γ_{20}. This procedure is equivalent to incorporating a normalized bandpass limiter between the preamplifier and the TWT amplifier in Figure C-1. The resulting model is shown in Figure C-2. The normalized limiter consists of an amplifier of gain G_o preceding the limiter, followed by another amplifier of reciprocal gain $1/G_o$. The gains of these two amplifiers are such that the power levels at the output of the preamplifier and at the input to the TWT amplifier are the same as in Figures C-1 and C-2.

Appendix A shows that γ_1 and γ_2 can be determined by solving two equations [Eqs. (A-34) and (A-38)]:

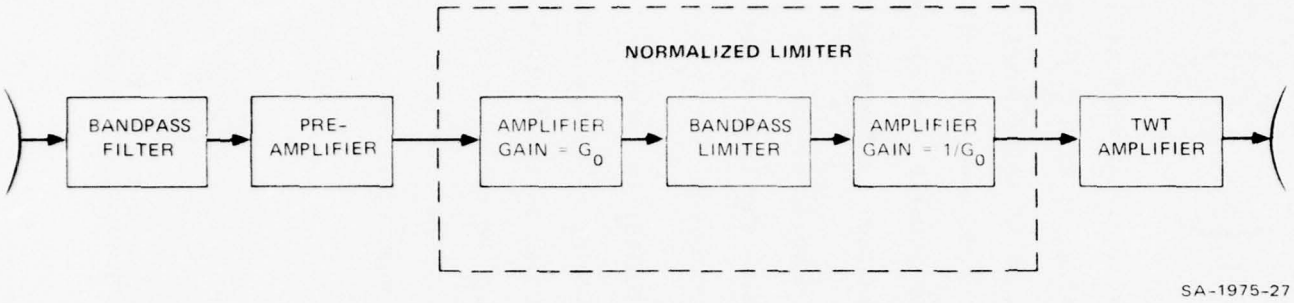

FIGURE C-2 MODEL FOR THE SATELLITE REPEATER WITH A NORMALIZED LIMITER

$$\frac{1}{\gamma_1} + \frac{1}{\gamma_2} = \frac{\sqrt{2\pi}}{\alpha} \tag{C-4}$$

$$\frac{1}{\gamma_1} \cdot {}_1F_1\left(\frac{1}{2}, 2, -\frac{P_{io}}{\gamma_1^2}\right) + \frac{1}{\gamma_2} \cdot {}_1F_1\left(\frac{1}{2}, 2, -\frac{P_{io}}{\gamma_2^2}\right) = \frac{\sqrt{2\pi}}{\alpha} \cdot \sqrt{\frac{P_{o1}}{P_{io}}} \quad . \tag{C-5}$$

Equation (C-4) is obtained by requiring that at low input levels the output power level should increase linearly with the input power, while Eq. (C-5) specifies an output power P_{o1} at an input power P_{io}. Since, for the normalized limiter the maximum output power is 0 dBW, we have $\alpha^2 = \pi^2/8$ [Eq. (A-29)]. Specifying an output power P_{o1} at an input power $P_{io} = P_{omax} = 0$ dBW (this corresponds, for example, to the normalized output $P_{o1}/P_{omax} = -4$ dB at 0-dB normalized input power level for the limiter characteristic shown in Figure A-7), we can determine the limiter parameters γ_{10} and γ_{20} (referenced to 0-dBW output) by solving Eqs. (C-4) and (C-5).

In Figure C-2 the limiter is preceded by two amplifiers of total gain $G_a \cdot G_o$. If we now define P_i to be the power at the input to the preamplifier, the power at the input to the limiter is then $G_a \cdot G_o P_i$. This corresponds to simply dividing the values of γ_{10} and γ_{20} by $G_a \cdot G_o$, as can easily be seen from Eq. (C-3). Thus, in terms of the power level at the input to the preamplifier in Eqs. (C-1) and (C-2), the limiter parameters γ_1 and γ_2 are given by

$$\gamma_1^2 = \frac{\gamma_{10}^2}{G_a \cdot G_o} \quad , \qquad \gamma_2^2 = \frac{\gamma_{20}^2}{G_a \cdot G_o} \quad . \tag{C-6}$$

Here γ_{10}^2 and γ_{20}^2 are the values of γ_1^2 and γ_2^2 for $G_a = G_o = 0$ dB.

b. Determination of G_o

In Figure C-2 the maximum power output of the bandpass limiter is 0 dBW, which is achieved at large input power levels. This power output

will yield the maximum satellite effective radiated power P_{max}. Since P_{max} is given by

$$P_{max}(dBW) = 0(dBW) - G_o(dB) + G_{twt}(dB) + G_{st}(dB) \quad ,$$

we obtain, in ratios for G_o, the expression

$$G_o = \frac{G_{twt} \cdot G_{st}}{P_{max}} \quad , \tag{C-7}$$

where

G_{st} = satellite transmitting antenna gain

G_{twt} = gain of the TWT amplifier.

In SYSCON, γ_1 and γ_2 are determined from Eqs. (C-6) and (C-7). First, γ_{10} and γ_{20} are calculated in the subroutine PINOUT by solving Eqs. (C-4) and (C-5) and normalizing the maximum power output of the limiter to 0 dBW. This corresponds, for example, to approximating the power transfer characteristic of Figure A-7 normalized by a maximum power output of 0 dBW. The ratio P_{ol}/P_{io} in Eq. (C-5) then represents the power back-off at 0-dB normalized input.

4. Initialization

The program is initiated by specifying as inputs the satellite terminal characteristics listed in Table C-1 and assigning specific frequencies and powers (ERP) to the n links, either directly or from an initialization plan. The bandwidth W of the repeater is defined as the frequency difference between the highest and the lowest assigned frequency links plus half the sum of the data rates of these two links. The initial frequency plan for the remaining carriers is then a proportionate spacing based on the data rate of each link. Fixing the end points of the repeater bandwidth

Table C-1

LISTINGS OF THE INPUT PARAMETERS REQUIRED IN SYSCON

Parameters	Units	Description
Satellite parameters		
G_{st}	dB	Satellite transmitting antenna gain
G_{sr}	dB	Satellite receiving antenna gain
G_a	dB	Preamplifier gain
G_{twt}	dB	TWT amplifier gain
P_{max}	dBW	Satellite ERP
T_s	^oK	Satellite noise temperature
W	MHz	Repeater bandwidth
γ_1, γ_2	W	Limiter parameters*
f_{offset}	GHz	Frequency translation for down-link transmission
f_{mid}	GHz	Midband frequency (down-link)
d	km	Distance between ground terminal and satellite
L	dB	Miscellaneous link losses
n		Number of links
Link parameters		
G_{ri}/T_{ri}	$dB/^oK$	Figure of merit of the i^{th} receiver
R_i	kbps	Bit rate of the i^{th} link
f_i	GHz	Frequency of the i^{th} link
S_{ti}	dBW	ERP of the i^{th} transmitter

*If γ_1 and γ_2 are not known, they can be determined in Subroutine PINOUT.

reduces the number of variables in the frequency optimization by two. The frequency variable used in the optimization procedure is the difference between successive frequencies, i.e., $\Delta f_1 = f_1 - f_o$, $\Delta f_2 = f_2 - f_1$, and so on.

The ERP are assigned in proportion to the ratio of the data rate and receiving-terminal-gain-to-temperature ratio (G/T) such that the sum of the power levels equals a constant. Thus, if there are n links, the ERP for the i^{th} link is determined as

$$s_{ti} = \frac{R_i/(G/T)_i}{\sum_{k=1}^{n} R_k/(G/T)_k} S_{to} \quad , \tag{C-8}$$

where S_{to} is the constant representing the equivalent power of a single carrier. The program is set up so that any desired value can be assigned to S_{to}.

A subroutine, IPERM, is included in SYSCON to run the program with the different possible orderings of the links in the repeater.

Example

Suppose we want to determine the value of S_{to} to yield a given value, say 1/p, for P_{in}/P_{omax} in Figure A-7. Thus, we require

$$P_{in} = \frac{P_{omax}}{p} = \frac{P_{max}}{p \cdot G_{st} \cdot G_{twt}} \quad ,$$

where P_{omax} is the maximum output power of the limiter in Figure C-1. The power at the input to the limiter P_{in} and the transmitter ERP S_{to} are related by the range equation

$$P_{in} = S_{to} \frac{G_{sr} \cdot G_a \cdot \lambda^2 \cdot L}{(4\pi d)^2} \quad .$$

Thus, S_{to} is given by:

$$S_{to} = \frac{P_{max}}{G_{sr} \cdot G_a \cdot G_{twt} \cdot G_{st} \cdot L \cdot p} \cdot \left(\frac{4\pi d}{\lambda}\right)^2 \quad ,$$

or, in decibels,

$$S_{to}(\text{dBW}) = P_{max} - G_{sr} - G_{st} - G_{twt} - G_a - L - p + 20 \log \left(\frac{4\pi d}{\lambda}\right) \quad .$$

For an up-link frequency of 8.0 GHz and a synchronous satellite with the following repeater characteristics

G_{sr}	16.8	dB	Satellite receiving antenna gain
G_{st}	17.0	dB	Satellite transmitting antenna gain
P_{max}	13.0	dBW	Satellite ERP
G_a	69.0	dB	Gain of the preamplifier preceding the limiter
L	1.0	dB	Miscellaneous link losses
G_{twt}	27.0	dB	Gain of the TWT amplifier

we obtain

$$S_{to} = 74 \text{ dBW} \quad ,$$

if p = 10 dB, i.e., P_{in}/P_{omax} equal to -10 dB is required.

5. Expression for the Error Probability

a. General

The general expression for the bit-error probability at the output of the i^{th} channel is given by [Appendix B, Eq. (B-20)]

$$P_{ei} = \frac{1}{2}\left[1 - \text{erf}\left(r_i/\sqrt{2}\right)\right] \quad , \qquad \text{(C-9)}$$

where

$$r_i^2 = \frac{\rho_i^2}{1 + \sum_{\substack{k=1 \\ k \neq 1}}^{n} \rho_{ik}^2 S_{ik} + \sum_{j=1}^{m} \hat{\rho}_{ij}^2 \hat{S}_{ij}} \qquad \text{(C-10)}$$

represents the equivalent SNR or $2E/n_o$ at the output of the i^{th} channel.

The SNRs ρ_i^2, ρ_{ik}^2, and $\hat{\rho}_{ij}^2$ at the receiver can be determined by considering the down-link transmission of the signals:

$$\rho_i^2 = \frac{2P_r \cdot \left(G_{ri}/T_{ri}\right) \cdot A_i^2}{K\left[1 + \frac{\pi}{16} T_s \frac{P_r \cdot \left(G_{ri}/T_{ri}\right)}{P_t}\right] R_i} \approx \frac{2P_r \cdot \left(G_{ri}/T_{ri}\right) \cdot A_i^2}{K R_i} \qquad \text{(C-11)}$$

$$\rho_{ik}^2 = \frac{2P_r \cdot \left(G_{ri}/T_{ri}\right) \cdot A_k^2}{K\left[1 + \frac{\pi}{16} T_s \frac{P_r \cdot \left(G_{ri}/T_{ri}\right)}{P_t}\right] R_i} \approx \frac{2P_r \cdot \left(G_{ri}/T_{ri}\right) \cdot A_k^2}{K R_i} \qquad \text{(C-12)}$$

$$\hat{\rho}_{ij}^2 = \frac{2P_r \cdot \left(G_{ri}/T_{ri}\right) \cdot A_{m\,n\,p}^2}{K\left[1 + \frac{\pi}{16} T_s \frac{P_r \cdot \left(G_{ri}/T_{ri}\right)}{P_t}\right] R_i} \approx \frac{2P_r \cdot \left(G_{ri}/T_{ri}\right) \cdot A_{m\,n\,p}^2}{K R_i} \qquad \text{(C-13)}$$

and

$$P_t = \frac{\left(\gamma_1^2 + \sum_{i=1}^{n} s_i\right)}{\left[1 + \left(\frac{\gamma_1^2 + \sum_{i=1}^{n} s_i}{\gamma_2^2 + \sum_{i=1}^{n} s_i}\right)^{1/2}\right]^2}, \qquad \text{(C-14)}$$

where

P_r = satellite ERP referenced to the ground terminal

G_{ri}/T_{ri} = figure of merit of the i^{th} receiver

K = Boltzman's constant

T_s = satellite noise termperature in degrees Kelvin

s_i = power of the i^{th} signal at the repeater input

γ_i^2 = limiter parameter

R_i = bit rate of the quadriphase signal

A_i = amplitude of the i^{th} signal at the limiter output

A_k = amplitude of the k^{th} signal at the limiter output

$A_{m\ n\ p}$ = amplitude of the third-order cross product generated by the mixing of signals on links m, n, and p.

Here the A coefficients are identical with the h coefficients discussed in Appendix A. They are defined as:

$$A_{p_1 p_2 \cdots p_n} = \frac{1}{2}\left[\int_0^\infty \prod_{i=1}^{n} J_{p_i}(va_i)\left\{\exp\left[-\frac{v^2\left(\sigma^2+\gamma_1^2\right)}{2}\right]\frac{dv}{v} + \exp\left[-\frac{v^2\left(\sigma^2+\gamma_2^2\right)}{2}\right]\frac{dv}{v}\right\}\right] , \quad \text{(C-15)}$$

where a_i is the ampiitude of the i^{th} signal at the limiter input, and σ^2 is the noise power at the input to the limiter. The approximations in Eqs. (C-11) through (C-13) refer to the fact that in FDMA the retransmitted up-link noise is usually negligible compared to the down-link noise.

The satellite ERP P_r referenced to the ground terminal and the i^{th} signal power s_i at the input to the satellite repeater are determined as follows:

$$P_r = P_{max} \cdot \frac{\lambda_u^2 \cdot L_d}{(4\pi d)^2} \qquad \text{(C-16)}$$

and

$$s_i = s_{ti} \cdot G_{sr} \frac{\lambda_d^2 \cdot L_d}{(4\pi d)^2} \quad , \qquad \text{(C-17)}$$

where

P_{max} = satellite ERP

λ = wavelength of the midband frequency for down-link transmission

L_d = miscellaneous losses (down-link)

d = distance between the ground station and the satellite

G_{sr} = satellite receiving antenna gain

s_{ti} = ERP of the i^{th} ground terminal.

By combining Eqs. (B-38) through (B-48) in Appendix B, the following expressions are obtained for S_{ik} and $\hat{S}_{ij}$ in Eq. (C-10):

$$S_{ik} = \frac{1}{T_i} \int_o^{T_{min}} \left(1 - \frac{|\tau|}{\tau_i}\right)\left(1 - \frac{|\tau|}{\tau_k}\right)\left(\cos \Delta\omega_k \tau\right) d\tau \quad ,$$

$$T_{min} = \min T_\ell, \text{ for } \ell = i,k \qquad \text{(C-18)}$$

$$\hat{S}_{ij} = \frac{1}{T_i} \int_o^{T_{min}} \left(1 - \frac{|\tau|}{T_m}\right)\left(1 - \frac{|\tau|}{T_n}\right)\left(1 - \frac{|\tau|}{T_p}\right)\left(1 - \frac{|\tau|}{T_i}\right) \cos\left(\Delta\omega_j \tau\right) d\tau \quad ,$$

$$T_{min} = \min T_\ell, \text{ for } \ell = i,m,n,p \quad , \qquad \text{(C-19)}$$

where

$$\Delta\omega_k = \omega_k - \omega_i$$

$$\Delta\omega_j = \omega_j - \omega_i$$

$T_i = \frac{2}{R_i}$ = bit interval of the i^{th} link

R_i = bit rate of the i^{th} link

ω_i = radian frequency of the i^{th} link

ω_k = radian frequency of the k^{th} link

ω_j = radian frequency of the j^{th} cross product.

In Eqs. (C-18) and (C-19) the indices i, m, n, and p indicate the links involved, while the index j is an index on the intermodulation product generated by signals from links m, n, and p.

Three subroutines are used in SYSCON to calculate the error rate by Eq. (C-9): AMP, SPECOLP, and ANORM. Subroutine AMP calculates the amplitudes of the signals and the cross products at the output of the bandpass limiter; SPECOLP determines the power contribution at the output of the i^{th} receiver from all the other FDMA signals (adjacent-channel interference) and third-order cross products; and, finally, ANORM calculates the bit-error rate for each channel by using Eq. (C-9).

b. Amplitudes of Limiter Output Signals and Intermodulation Components

Program AMP calculates the amplitudes of the signals and intermodulation products by Eq. (C-15). The infinite integral is approximated by a finite integral in the interval from 0 to U, where U is the upper limit of integration and is determined such that the truncation error in the integral is negligible. Equation (C-15) is first normalized through substitution of the following

$$c_2 = \frac{\sigma^2 + \gamma_1^2}{2} \quad , \qquad c_3 = \frac{\sigma^2 + \gamma_2^2}{2} \quad ,$$

where $c = \min (c_2, c_3)$. This yields

$$A_{p_1, p_2 \cdots p_n} = \frac{1}{2} \int_o^U \prod_{i=1}^{n} J_{p_i}\left(a_i \cdot z/\sqrt{c}\right) \left[\exp\left(-\frac{c_2}{c} z^2\right) + \exp\left(-\frac{c_3}{c} z^2 \quad \frac{dz}{z}\right)\right] \quad . \qquad \text{(C-20)}$$

Since

$$\left| \prod_{i=1}^{n} J_{p_i}\left(\frac{a_i}{\sqrt{c}} z\right) \right| \leq 1 \quad ,$$

and at $z = 4$

$$\frac{e^{-z^2}}{4} = \frac{e^{-16}}{4} = 2.85 \times 10^{-8} \quad ,$$

the integral converges to a limit very fast as z increases. It was found that, under all circumstances, the contribution of the integral in the region $z = 4$ to ∞ is typically of the order of 0.0001 percent. So the infinite integral in Eq. (C-20) can be approximated by integration in the region $z = 0$ to 4. Thus, $U = 4$ in Eq. (C-20).

The Bessel functions J_o and J_1 in Eq. (C-20) can be calculated from their polynomial approximations,[12]

$$-3 \leq x \leq 3$$

$$J_o(x) = 1 - 2.24999\ 97\ (x/3)^2 + 1.26562\ 08(x/3)^4$$

$$- 0.31638\ 66\ (x/3)^6 + 0.04444\ 79\ (x/3)^8$$

$$- 0.00394\ 44(x/3)^{10} + 0.00021\ 00(x/3)^{12} + \epsilon$$

$$|\epsilon| < 5 \times 10^{-8} \qquad \text{(C-21)}$$

$$3 \leq x < \infty$$

$$J_o(x) = x^{-1/2} f_o \cos \theta_o \qquad Y_o(x) = x^{-1/2} f_o \sin \theta_o$$

$$f_o = 0.79788\ 456 - 0.00000\ 077(3/x) - 0.00552\ 740(3/x)^2$$

$$- 0.00009\ 512(3/x)^3 + 0.00137\ 237(3/x)^4$$

$$- 0.00072\ 805(3/x)^5 + 0.00014\ 476(3/x)^6 + \epsilon$$

$$|\epsilon| < 1.6 \times 10^{-8} \qquad \text{(C-22)}$$

$$\theta_o = x - 0.78539\ 816 - 0.04166\ 397(3/x)$$

$$- 0.00003\ 954\ (3/x)^2 + 0.00262\ 573(3/x)^3$$

$$- 0.00054\ 125(3/x)^4 - 0.00029\ 333(3/x)^5$$

$$+ 0.00013\ 558(3/x)^6 + \varepsilon$$

$$|\varepsilon| < 7 \times 10^{-8} \qquad \text{(C-23)}$$

$$-3 \leq x \leq 3$$

$$x^{-1} J_1(x) = \frac{1}{2} - 0.56249\ 985(x/3)^2 + 0.21093\ 573(x/3)^4$$

$$- 0.03954\ 289(x/3)^6 + 0.00443\ 319(x/3)^8$$

$$- 0.00031\ 761(x/3)^{10} + 0.00001\ 109(x/3)^{12} + \varepsilon$$

$$|\varepsilon| < 1.3 \times 10^{-8} \qquad \text{(C-24)}$$

$$J_1(x) = x^{-1/2} f_1 \cos \theta_1 \quad , \quad 3 \leq x < \infty$$

$$f_1 = 0.79788\ 456 + 0.00000\ 156(3/x) + 0.01659\ 667(3/x)^2$$

$$+ 0.00017\ 105(3/x)^3 - 0.00249\ 511(3/x)^4$$

$$+ 0.00113\ 653(3/x)^5 - 0.00020\ 033(3/x)^6 + \varepsilon$$

$$|\varepsilon| < 4 \times 10^{-8} \qquad \text{(C-25)}$$

$$\theta_1 = x - 2.35619\ 449 + 0.12499\ 612(3/x)$$

$$+ 0.00005\ 650(3/x)^2 - 0.00637\ 879(3/x)^3$$

$$+ 0.00074\ 348(3/x)^4 + 0.00079\ 824(3/x)^5$$

$$- 0.0029\ 166\ (3/x)^6 + \varepsilon$$

$$|\varepsilon| < 9 \times 10^{-8} \qquad \text{(C-26)}$$

and J_2 is calculated by the recurrence relationship

$$J_{\nu-1}(z) + J_{\nu+1}(z) = \frac{2\nu}{z} J_\nu(z) \quad . \qquad \text{(C-27)}$$

The finite integral of Eq. (C-20) is first divided into either two or four subintervals, depending upon the maximum value of $a_i/\sqrt{c}$; then each subinterval is evaluated by the 16-point Gaussian quadrature method.

The value of $a_i/\sqrt{c}$ in J_o and J_1 influences the accuracy with which the integral in Eq. (C-20) can be calculated by the Gaussian quadrature method. A larger value of $a_i/\sqrt{c}$ means J_o and J_1 will have more zero crossings in the interval (0,4). Hence a polynomial of higher degree is needed to approximate

$$\prod_{i=1}^{n} J_{p_1}\left(a_i z/\sqrt{c}\right) \quad ,$$

and hence more points will be needed in the Gaussian quadrature method. Subroutine AMP takes this into consideration. For $a_i/\sqrt{c} \leq 1$, the integral interval (0,4) is divided into two subintervals, (0,2) and (2,4). For $a_i/\sqrt{c} > 1$, the interval (0,4) is divided into four subintervals, (0,0.5), (0.5,1), (1,2), and (2,4). Each subinterval is then evaluated by the

16-point Gaussian quadrature formula and is added to give the final answer.

Subroutine AMP evaluates Eq. (C-20) with the aid of three subroutines:

FUNCTION AJO(X)--To calculate Bessel function J_o.

FUNCTION AJI(X)--To calculate Bessel function J_1.

SUBROUTINE QG16--To perform 16-point Gaussian quadrature integration.

Subroutine AMP has been thoroughly tested. Values of the integral calculated from this program were compared with results from an earlier SRI program that utilizes the Newton-Cotes integration formula. The results from these two programs were found to be in excellent agreement (to at least five figures). The program using the Gaussian quadrature method runs very much faster than the one using the Newton-Cotes formula.

c. Frequencies of the Cross-Product Components

Subroutine CALXSM is used in SYSCON to calculate the frequencies of all third-order intermodulation products. Note that there are two types of third-order cross products. These are generated at frequencies

$$2 f_i - f_j = f_{21}$$

and

$$f_i + f_j - f_k = f_{111} \quad .$$

The cross product at the frequency $2f_i - f_j$ is produced as a result of mixing of two signals at frequencies f_i and f_j, respectively. The cross

product at the frequency $f_i + f_j - f_k$ is generated as a result of mixing of three signals at frequencies f_i, f_j, and f_k.

d. Calculation of S_{ik} and $\hat{S}_{ij}$

Subroutine SPECOLP calculates the integrals in Eqs. (C-18) and (C-19). Note that Eq. (C-18) is a subset of Eq. (C-19), involving only two products instead of four. By multiplying out the four products in Eq. (C-18), $\hat{S}_{ij}$ can be expressed as a sum of four integrals

$$T_i \cdot \hat{S}_{ij} = \int_o^{T_{min}} \cos\left(\Delta\omega_j \tau\right) d\tau - \left(\frac{1}{T_m} + \frac{1}{T_n} + \frac{1}{T_p} + \frac{1}{T_i}\right) \int_o^{T_{min}} \tau \cos\left(\Delta\omega_j \tau\right) d\tau$$

$$+ \left(\frac{1}{T_m T_n} + \frac{1}{T_m T_p} + \frac{1}{T_m T_i} + \frac{1}{T_n T_p} + \frac{1}{T_n T_i} + \frac{1}{T_p T_i}\right) \int_o^{T_{min}} \tau^2 \cos\left(\Delta\omega_j \tau\right) d\tau$$

$$- \left(\frac{1}{T_m T_n T_p} \quad \frac{1}{T_m T_n T_i} \quad \frac{1}{T_n T_p T_i} \quad \frac{1}{T_m T_p T_i}\right) \int_o^{T_{min}} \tau^3 \cos\left(\Delta\omega_j \tau\right) d\tau$$

$$+ \frac{1}{T_m T_n T_p T_i} \int_o^{T_{min}} \tau^4 \cos\left(\Delta\omega_j \tau\right) d\tau$$

$$T_{min} = \min T_\ell, \text{ for } \ell = i,m,n,p \quad . \quad \text{(C-28)}$$

Each term can be integrated analytically. Table C-2 gives the expressions used in programming Eq. (C-28).

Table C-2

INTEGRALS USED IN THE SUBROUTINE SPECOLP

Integral	For $\Delta\omega\tau > 0$*	For $\Delta\omega\tau = 0$
$\int_0^{T_{min}} \cos(\Delta\omega\tau)d\tau$	$\frac{\sin\left(\Delta\omega T_{min}\right)}{\Delta\omega}$	T_{min}
$\int_0^{T_{min}} \tau\cos(\Delta\omega\tau)d\tau$	$\frac{\cos\left(\Delta\omega T_{min}\right)}{\Delta\omega^2} + \frac{T_{min}\sin\left(\Delta\omega T_{min}\right)}{\Delta\omega} - \frac{1}{\Delta\omega^2}$	$\frac{T_{min}^2}{2}$
$\int_0^{T_{min}} \tau^2\cos(\Delta\omega\tau)d\tau$	$\frac{2T_{min}\cos\left(\Delta\omega T_{min}\right)}{\Delta\omega^2} + \left(T_{min}^2 - \frac{2}{\Delta\omega^2}\right)\frac{\sin\left(\Delta\omega T_{min}\right)}{\Delta\omega}$	$\frac{T_{min}^3}{3}$
$\int_0^{T_{min}} \tau^3\cos(\Delta\omega\tau)d\tau$	$3\left(T_{min}^2 - \frac{2}{\Delta\omega^2}\right)\frac{\cos\left(\Delta\omega T_{min}\right)}{\Delta\omega^2} + T_{min}\left(T_{min}^2 - \frac{6}{\Delta\omega^2}\right)\frac{\sin\left(\Delta\omega T_{min}\right)}{\Delta\omega} + \frac{6}{\Delta\omega^4}$	$\frac{T_{min}^4}{4}$
$\int_0^{T_{min}} \tau^4\cos(\Delta\omega\tau)d\tau$	$4T_{min}\left(T_{min}^2 - \frac{6}{\Delta\omega^2}\right)\frac{\cos\left(\Delta\omega T_{min}\right)}{\Delta\omega^2} + \left[T_{min}^4 - \frac{12}{\Delta\omega^2}\left(T_{min}^2 - \frac{2}{\Delta\omega^2}\right)\right]\frac{\sin\left(\Delta\omega T_{min}\right)}{\Delta\omega}$	$\frac{T_{min}^5}{5}$

* $\Delta\omega$ here is the same as $\Delta\omega_j$ in Eq. (C-28).

The variable inputs to this subroutine are the $\Delta\omega_j$ and the indices. As $\Delta\omega_j$ approaches zero, the integrals simplify, with the cosine terms approaching one. For values of $\Delta\omega_j T_{min}$ close to zero, the expressions shown in Column 3 of Table C-2 are used.

To find the expression for S_{ik} it is necessary only to set $1/T_p$ and $1/T_n$ equal to zero in Eq. (C-28).

Equation (C-28) is used as follows for the various types of third-order cross products:

- If the cross product under consideration is generated as a result of mixing of signals other than the desired signal, Eq. (C-28) is valid for determining the spectrum overlap resulting from the cross product of the type $f_m + f_n - f_p$. For the cross product of the type $2f_m - f_n$, we need only to set $1/T_p$ equal to zero in Eq. (C-28).
- If the cross product under consideration is generated as a result of mixing of signals involving the desired signal, then, for the type $f_m + f_n - f_p$ cross product, $\hat{S}_{ij}$ is determined by setting either $1/T_p$, $1/T_m$, or $1/T_n$ equal to zero (depending upon which of the three indices m, n, p is equal to i). For the cross product of the type $2f_m - f_n$, we set $1/T_p$ equal to zero, as explained above, and also either $1/T_m$ or $1/T_n$ equal to zero (depending upon which of the two indices m or n is equal to i). This procedure is necessary, as explained in connection with Eq. (B-47), when considering the effects of cross products at the receiver that are produced because of mixing of signals with the desired signal.

6. Approach for Selecting Power and Frequency

The approach taken for optimization in SYSCON is to optimize the norm N_a or N_b first with respect to either the frequency or the power, by holding one of them fixed, and then to repeat the procedure on the parameter that was held fixed. The reason for doing this is that frequency and power are easily separable in Eq. (C-10). The SNRs ρ_i^2, ρ_{ik}^2, and $\hat{\rho}_{ij}^2$ are functions of the transmitter ERPs, while S_{ik} and $\hat{S}_{ij}$ are dependent on their frequencies.

The program is initiated by first assigning specific frequencies and powers to the n links, either directly or from the initialization plan discussed in Section 4. The probability of error for each of the n links is then calculated. The next step is to minimize either of the two norms, which can be selected at the start of the program.

The problem of minimizing the norm is equivalent to finding the minimum of a function of n variables. A standard technique for solving a problem of this type is the method of steepest descent. It consists of picking a point, calculating the partial derivatives at this point, and proceeding in the direction of the steepest slope by a specified amount. After the step has been taken, the function is evaluated to see whether it is less than its previous value. If it is less, the procedure is continued; if not, a smaller step is taken. If a minimum exists, it will be found eventually.

The algorithm used in SYSCON for both power and frequency optimization is an improved version of the steepest descent method.

a. Description of the Optimization Approach

Methods of minimization of a function of several variables can be divided into two groups: direct search methods, which do not depend explicitly on evaluation or estimation of the gradient vector of the

objective function, and gradient methods, which require derivatives. Since no derivatives are required by the direct search methods, they are applicable to functions with discontinuous derivatives. If derivatives can be evaluated, the gradient methods are usually far more efficient. In the satellite FDMA problem, analytic expressions for the derivatives of the norm exist; therefore, only gradient methods for minimization of the norm were considered.

In the discussions below, $U(\tilde{\Phi})$ is a function of k variables, $[U(\tilde{\Phi})]_{min}$ is the minimum value of $U(\tilde{\Phi})$, and j stands for the j^{th} direction.

1) The Newton Method

If we expand $U(\tilde{\Phi} + \Delta\tilde{\Phi})$ in a Taylor series about $\tilde{\Phi}$, we have

$$U(\tilde{\Phi} + \Delta\tilde{\Phi}) = U(\tilde{\Phi}) + \tilde{\nabla}U^{T}(\tilde{\Phi})\Delta\tilde{\Phi} + \ldots \quad , \tag{C-29}$$

where $\tilde{\nabla}U$ is the gradient vector. Differentiating the Taylor series again, we obtain

$$\tilde{\nabla}U(\tilde{\Phi} + \Delta\tilde{\Phi}) = \tilde{\nabla}U(\tilde{\Phi}) + \tilde{H}\Delta\tilde{\Phi} + \ldots \quad , \tag{C-30}$$

where H, the Hessian matrix, is given by

$$\tilde{H} = \tilde{\nabla}\left(\tilde{\nabla}U^{T}\right) \quad . \tag{C-31}$$

For $\tilde{\Phi} + \Delta\tilde{\Phi}$ to be the minimizing point, $\tilde{\Phi}_{min}$, $\tilde{\nabla}U(\tilde{\Phi} + \Delta\phi)$ would be $\tilde{0}$, so, neglecting higher-order terms,

$$\tilde{\Delta}\Phi = -\tilde{H}^{-1}\tilde{\nabla}U \quad . \tag{C-32}$$

If we are dealing with a quadratic function, this incremental change will take us to the minimum in only one iteration.

When U is not quadratic, one can try the iterative scheme

$$\tilde{\Phi}^{j+1} = \tilde{\Phi}^{j} - \tilde{H}^{-1}\tilde{\nabla}U^{j} \quad , \tag{C-33}$$

where $\tilde{H}^{-1}$ is the inverse of the Hessian matrix at the j^{th} iteration. This scheme has, however, several disadvantages. $\tilde{H}$ must be positive definite; otherwise divergence could occur. In particular, $-\tilde{H}^{-1}\tilde{\nabla}U^{j}$ might not point downhill. Also, $\tilde{H}$ may be locally singular; if so, its inverse does not exist. This scheme was tried for the optimization of the norm. The computations of $\tilde{H}$, the second derivative matrix, and its inverse were very time consuming.

2) Steepest Descent

Instead of Eq. (C-33), one can try the iterative scheme

$$\tilde{\Phi}^{j+1} = \tilde{\Phi}^{j} + \alpha^{j}\tilde{s}^{j} \quad , \tag{C-34}$$

where $\tilde{s}^{j}$ is (hopefully) a "downhill" direction of search, and $\alpha^{j} > 0$ is the step size or a scale factor chosen to minimize $U(\tilde{\Phi}^{j} + \alpha^{j}\tilde{s}^{j})$.

The most obvious choice for $\tilde{s}^{j}$ is the steepest-descent direction at $\tilde{\Phi}^{j}$. From Eq. (C-29), a first-order change in the objective function is given by

$$\Delta U = \tilde{\nabla}U^{T}\Delta\tilde{\Phi} \quad . \tag{C-35}$$

If $\Delta\tilde{\Phi} = \alpha^{j}\tilde{s}^{j}$, where $\alpha^{j} > 0$ is fixed and $\|\tilde{s}^{j}\| = 1$, it is easy to show that the $\tilde{s}^{j}$ minimizing ΔU or maximizing $-\Delta U$ is given by

AD-A047 044 STANFORD RESEARCH INST MENLO PARK CALIF F/G 17/2.1
INVESTIGATION OF THE USE OF FREQUENCY-DIVISION MULTIPLE ACCESS --ETC(U)
DEC 73 P C JAIN, V E HATFIELD, J K LEUNG DCA100-72-C-0033
UNCLASSIFIED NL

2 OF 2
ADA047044

END
DATE FILMED
1-78
DDC

$$\tilde{s}^j = - \frac{\tilde{\nabla} U^j}{\|\tilde{\nabla} U\|} \quad , \tag{C-36}$$

where $\| \cdot \|$ is the Euclidean norm defined as

$$\|\tilde{v}\| \triangleq \tilde{v}^T \tilde{v} = \left(\sum_i v_i^2 \right)^{1/2} \quad .$$

The s^j in Eq. (C-36) is the negative of the normalized gradient vector. Although $- \tilde{\nabla} U / \|\tilde{\nabla} U\|$ provides the greatest local change, success of the steepest descent method is highly dependent on the scaling factor α^j.

3) Algorithm Used in SYSCON for FDMA Optimization

The selected algorithm is a modified version of the steepest descent method. The objective function U corresponds to the norm N, and $\tilde{\Phi}$ is either the frequency or the input signal amplitudes. Equation (C-36) of the steepest descent method is modified as follows:

$$\tilde{s}^j = (1 - \beta) \frac{\tilde{\nabla} U^j}{\|\tilde{\nabla} U^j\|} + \beta \frac{\tilde{\nabla} U^{j-1}}{\|\tilde{\nabla} U^{j-1}\|} \quad , \tag{C-37}$$

to locate the direction of the minimum. Comparison of this $\tilde{s}^j$ with Eq. (C-36) shows that the gradient selected is the weighted sum of the two gradients. For $\beta = 0$ we obtain the same result as with the steepest descent method.

The step size α^j [in Eq. (C-34)] is first set to be proportional to $|\tilde{\Phi}^j|$, and is further adjusted automatically until a minimum is located along the $\tilde{s}^j$ direction; then

$$\tilde{\Phi}^{j+1} = \tilde{\Phi}^{j} + \alpha^{j}\tilde{s}^{j}$$

and

$$U\left(\tilde{\Phi}^{j+1}\right) \leq U\left(\tilde{\Phi}^{j}\right) \qquad \text{(C-38)}$$

is satisfied.

The iteration is repeated until some prescribed stopping criterion is satisfied. The stopping criteria consist of:

- The maximum number of allowable iterations has been reached.
- Either one of two inequalities has been satisfied,

$$\left|U\left(\tilde{\Phi}^{j+1}\right) - U\left(\tilde{\Phi}^{j}\right)\right| \leq \epsilon_1$$

$$\left|\left\|\tilde{\Phi}^{j+1} - \tilde{\Phi}^{j}\right\|\right| \leq \epsilon_2 \quad ,$$

where ϵ_1 and ϵ_2 have prescribed values.

A simplified flow chart of the optimization Subroutine STEEP is shown in Figure C-3 and is discussed in Volume One, Section IV-E.

7. Derivatives of the Norm

For power and frequency optimization, we need the derivatives of the norm with respect to the signal amplitudes and frequency differences.* Thus, if norm N_a is used, we need to determine

---

*As mentioned in Section 4, the variable used in frequency optimization is the difference between successive frequencies, i.e., $\Delta f_1 = f_1 - f_o$, $\Delta f_2 = f_2 - f_1$, and so on, instead of absolute frequencies f_1, f_2, and so on. This procedure reduces the number of variables in the optimization procedure by two.

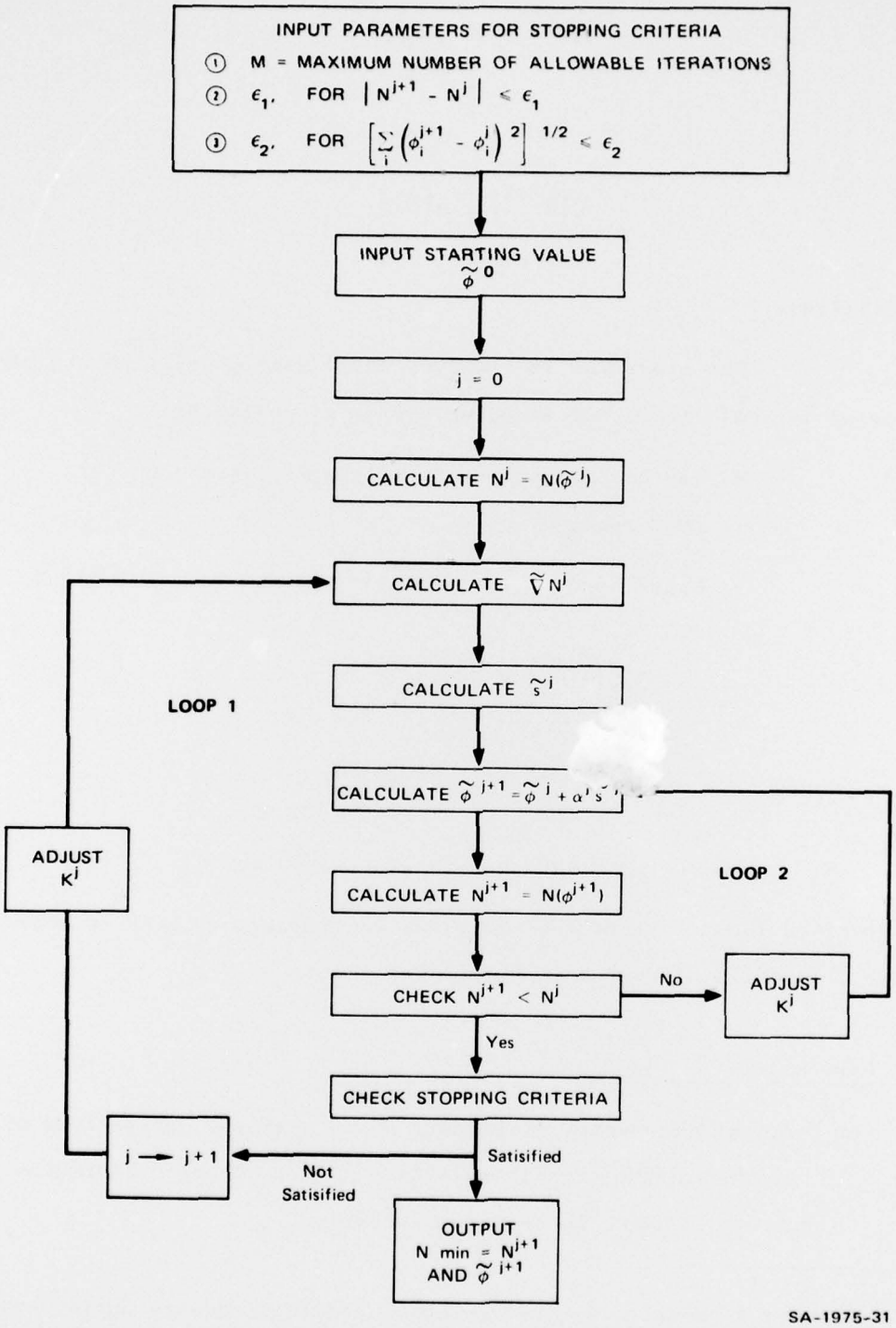

FIGURE C- 3 SIMPLIFIED FLOW CHART OF THE OPTIMIZATION PROGRAM STEEP

$$\frac{\partial N_a}{\partial a} = \sum_{i=1}^{n} \frac{\partial P_{ei}}{\partial a} \quad , \tag{C-39}$$

and

$$\frac{\partial N_a}{\partial \Delta f} = \sum_{i=1}^{n} \frac{\partial P_{ei}}{\partial \Delta f} \quad . \tag{C-40}$$

Here a and Δf represent, respectively, the desired amplitude and frequency differences.

a. Determination of $\partial P_{ei}/\partial a$

It can easily be shown from Eq. (C-9) that

$$\frac{\partial P_{ei}}{\partial a} = \frac{e^{-\rho_i^2/2(1+h)}}{\sqrt{2\pi}} \left[\frac{1}{2} \cdot \frac{\rho_i}{(1+h)^{3/2}} \frac{\partial h}{\partial a} - \frac{1}{(1+h)^{1/2}} \frac{\partial \rho_i}{\partial a} \right] \quad , \tag{C-41}$$

where

$$h = \sum_{\substack{k=1 \\ k \neq i}}^{n} \rho_{ik}^2 S_{ik} + \sum_{j} \hat{\rho}_{ij}^2 \hat{S}_{ij} \quad , \tag{C-42}$$

and

$$\frac{\partial h}{\partial a} = 2 \sum_{\substack{k=1 \\ k \neq i}}^{n} S_{ik} \frac{\partial \rho_{ik}}{\partial a} + 2 \sum_{j} \hat{S}_{ij} \frac{\partial \hat{\rho}_{ij}}{\partial a} \quad . \tag{C-43}$$

The derivatives of the SNRs with respect to signal amplitude can be expressed in terms of the corresponding derivatives of the limiter output amplitudes, by Eqs. (C-11) through (C-13). Thus, in general, we would require the derivatives $\partial A_i/\partial a$, $\partial A_k/\partial a$, and $\partial A_{m\,n\,p}/\partial a$, which,

in turn, can be calculated from Eq. (C-15). Since derivatives of Bessel functions can be expressed in terms of other Bessel functions, they lead to integrals similar to Eq. (C-15) and can be evaluated by using the approach discussed in the calculation of Eq. (C-20). In SYSCON the derivative of the norm N_a or N_b with respect to the signal amplitudes is calculated by evaluating the analytic expressions in Subroutine DNORMA.

b. Determination of $\partial P_{ei}/\partial \Delta f$

From Eq. (C-9) we can derive the following expression:

$$\frac{\partial P_{ei}}{\partial \Delta f} = \frac{1}{2} \cdot \frac{e^{-\rho_i^2/2(1+h)}}{\sqrt{2\pi}} \cdot \frac{\rho_i}{(1+h)^{3/2}} \cdot \frac{\partial h}{\partial \Delta f} \quad , \tag{C-44}$$

where h is defined by Eq. (C-43) and

$$\frac{\partial h}{\partial \Delta f} = \sum_{\substack{k=1 \\ k \neq i}}^{n} \rho_{ik}^2 \frac{\partial S_{ik}}{\partial \Delta f} + \sum_j \hat{\rho}_{ij}^2 \frac{\partial \hat{S}_{ij}}{\partial \Delta f} \quad . \tag{C-45}$$

The derivatives of Eq. (C-45) can also be expressed as

$$\frac{\partial S_{in}}{\partial \Delta f} = \frac{\partial S_{ik}}{\partial \Delta \omega_k} \cdot \frac{\partial \Delta \omega_k}{\partial \Delta f} \tag{C-46}$$

and

$$\frac{\partial \hat{S}_{ij}}{\partial \Delta f} = \frac{\partial \hat{S}_{ij}}{\partial \Delta \omega_j} \cdot \frac{\partial \Delta \omega_j}{\partial \Delta f} \quad . \tag{C-47}$$

Analytic expression for the derivatives in Eqs. (C-46) and (C-47) can be developed from Eqs. (C-18) and (C-19). In SYSCON, the derivatives of the norm N_a or N_b with respect to the frequency differences are calculated in Subroutine DNORMF.

8. Summary

A simplified conceptual flow chart diagram of SYSCON is shown in Figure C-4. The required input data are identified. The satellite and terminal parameters are those given in Table C-1. At the start of the program it is essential to provide the initial ordering of the links in the satellite repeater, as well as selection of the norm and the indication whether optimization of the norm is desired. Also necessary is the information whether other possible combinations of the links are to be considered.

If the limiter parameters γ_1 and γ_2 are not given in the input data, they are determined in Subroutine PINOUT. If they are known, this procedure is bypassed.

Next, the program determines the initial starting values for the ERPs and the up-link frequencies of the transmitters. Three options are available. First, the values and frequencies can be provided in the input data. Second, they can be determined from the initialization plan discussed in Section 4. A third option allows the possibility of providing only the values for the transmitter ERPs at the input; the initial frequency assignment is then assumed to be uniform within the satellite repeater.

The program then calculates the probability of error P_{ei} for each link by using Subroutines AMP, SPECOLP, and ANORM and also determines the value of the selected norm. If minimization of the norm was indicated at the input, it is performed next in Subroutine STEEP. The order of optimization (i.e., power first and then frequency, or vice versa) and the number of optimizations must be provided at the input. Subroutine STEEP (Figure C-3) is used for both power and frequency optimization. The values for the stopping criteria are already included in the program, but they can easily be changed if desired. The values used in the program are:

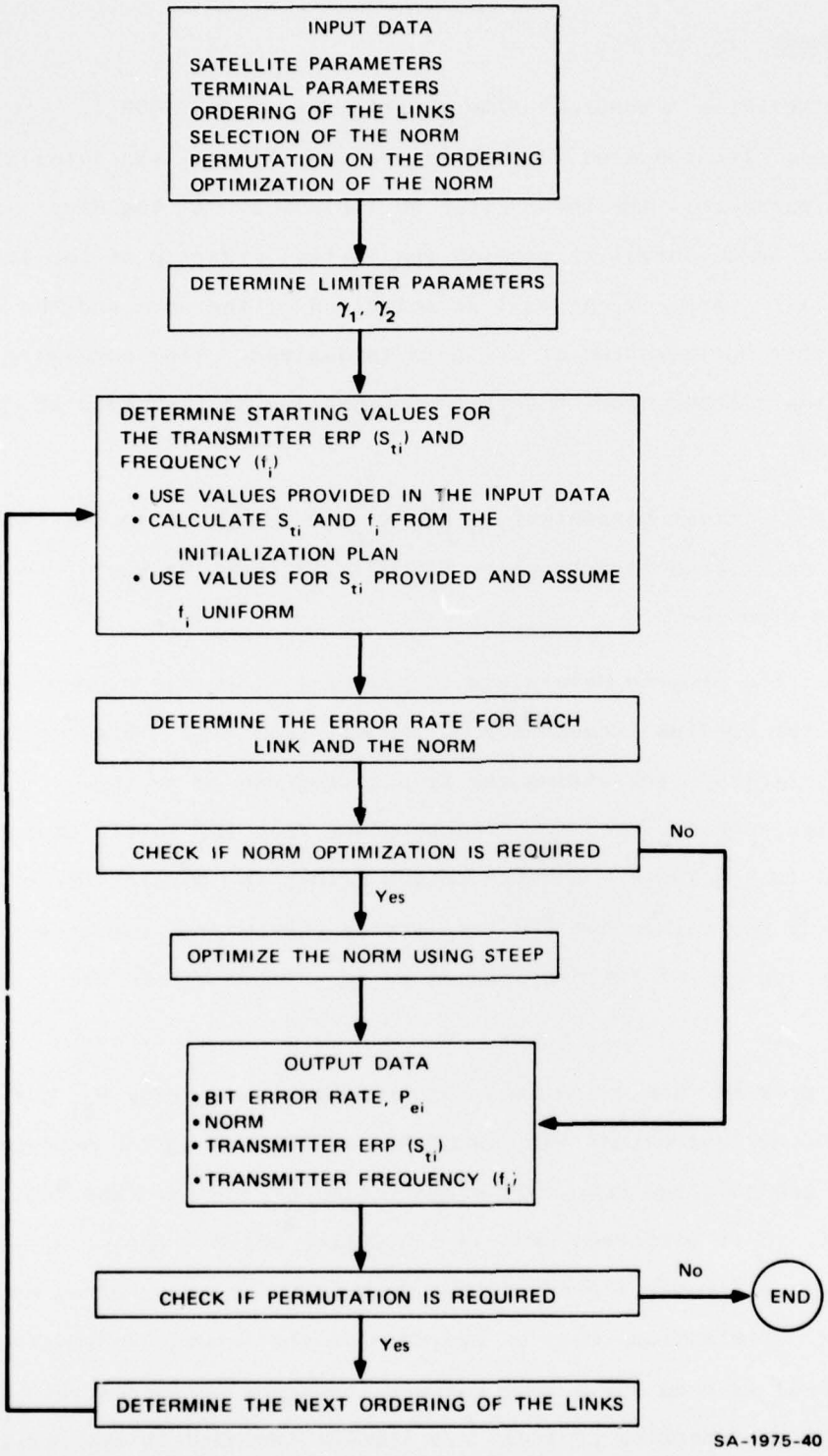

FIGURE C-4 SIMPLIFIED FLOW CHART OF SYSCON

Number of iterations $M = 10$

$$\epsilon_1 = 10^{-8}$$

$$\epsilon_2 = 0.001 \times \sum_{i=1}^{n} |\tilde{\phi}_i^o| \quad .$$

At the end of each optimization (power or frequency) the values of P_{ei}, S_{ti}, f_i, and the norm are printed.

After the last optimization, the program can be exercised again with the next combination of the links, if that is desired. The possible combinations are determined in Subroutine IPERM.

The numerical results obtained by using SYSCON are discussed in Volume One.

REFERENCES

1. W. Magnus, F. Oberhettinger, and R. P. Soni, Formulas and Theorems for the Special Functions of Mathematical Physics (Springer, New York, 1966), p. 418.

2. M. Abramowitz and I. A. Stegun, eds., Handbook of Mathematical Functions with Formulas, Graphs, and Mathematical Tables (Dover, New York, 1965), p. 486.

3. M. Abramowitz and I. A. Stegun, eds., Handbook of Mathematical Functions with Formulas, Graphs, and Mathematical Tables (Dover, Publications Inc., New York, 1965), p. 504.

4. C. R. Cahn, "Crosstalk Due to Finite Limiting of Frequency-Multiplexed Signals," Proc., IRE, Vol. 48, pp. 53-59 (January 1960).

5. "777 Communication Subsystem Reconfiguration Study," Final Report, Contract F04701-71-C-0380, TRW Systems (10 December 1971).

6. W. B. Davenport, Jr., "Signal-to-Noise Ratios in Bandpass Limiters," J. Appl. Phys., Vol. 24, pp. 720-727 (June 1953).

7. J. J. Jones, "Hard-limiting of Two Signals in Random Noise," IEEE Trans. Information Theory, Vol. IT-9, pp. 34-42 (January 1963).

8. P. D. Shaft, "Limiting of Several Signals and Its Effect on Communication System Performance," IEEE Trans. Commun. Technol., Vol. COM-13, pp. 504-512 (September 1965).

9. M. Gyi, "Some Topics on Limiters and FM Demodulators," Report SEL 65-056, Stanford University, Stanford, California (July 1965).

10. P. C. Jain, "Limiting of Signals in Random Noise," IEEE Trans. Information Theory, pp. 332-340 (May 1972).

11. E. Parzen, Modern Probability Theory and Its Application (John Wiley and Sons, Inc., New York, 1960), p. 402, Eq. (3.12)..

12. Abramowitz and Stegun, op. cit., p. 369.

Security Classification

DOCUMENT CONTROL DATA - R & D

(Security classification of title, body of abstract and indexing annotation must be entered when the overall report is classified)

1. ORIGINATING ACTIVITY (Corporate author)	2a. REPORT SECURITY CLASSIFICATION
Stanford Research Institute	Unclassified
	2b. GROUP

3. REPORT TITLE

Investigation of the Use of Frequency-Division Multiple Access for Application with a Mix of User Terminals, Vols. One, Two, and Three

4. DESCRIPTIVE NOTES (Type of report and inclusive dates)

Final Report

5. AUTHOR(S) (First name, middle initial, last name)

Pravin C. Jain, V. Elaine Hatfield, John K. Leung, D. Thomas Magill

6. REPORT DATE	7a. TOTAL NO. OF PAGES	7b. NO. OF REFS
December 1973	337	30

8a. CONTRACT OR GRANT NO.	9a. ORIGINATOR'S REPORT NUMBER(S)
DCA100-72-C-0033	SRI Project 1975
b. PROJECT NO.	
c.	9b. OTHER REPORT NO(S) (Any other numbers that may be assigned this report)
d.	

10. DISTRIBUTION STATEMENT

DISTRIBUTION UNLIMITED

11. SUPPLEMENTARY NOTES	12. SPONSORING MILITARY ACTIVITY
	Defense Communications Agency System Engineering Facility Reston, Virginia 22070

13. ABSTRACT

This report presents the results of research performed to investigate the application of the frequency-division multiple-access (FDMA) technique for providing a mix of user terminals of differing characteristics--such as data rates, transmitter powers, and receiver sensitivities--with simultaneous access capability to a limiting satellite repeater. A computer program (SYSCON) has been developed to model a PSK/FDMA satellite communication system and to optimize its performance in operation with a mix of user terminals, through selection of power and frequency plans. This capability is achieved through optimization of a norm defined as the weighted sum of the link error rates and representing the figure of merit or a measure of the system's communications performance with respect to both the power and the frequency of the links. The method of steepest descent is used for determining both power and frequency plans. It was found that through power and frequency control the limiting satellite repeater can be operated in the saturation region at substantially higher power levels (1-dB back-off) than is customary in practice.

To obtain the expression for the error rate at the input of the FDMA links, it was necessary to derive general analytic expressions for the limiter output signal, the intermodulation, and the noise components, when n signals are transmitted simultaneously through the satellite repeater. The expression for the bit error rate was then derived by assuming digital quadriphase modulation of the FDMA carriers and taking into consideration the presence of other FDMA carriers causing adjacent-channel interference, the intermodulation products generated in the limiter, and retransmitted satellite repeater noise, as well as receiver noise.

14 KEY WORDS	LINK A		LINK B		LINK C	
	ROLE	WT	ROLE	WT	ROLE	WT
Limiters, frequency-division multiple access, intermodulation products, error rate, steepest descent, time-division multiple access, spread-spectrum multiple access, power control, frequency control						

13. Abstract (Concluded)

A general comparison of the three major multiple-access alternatives--FDMA, TDMA, and SSMA--with respect to selected performance criteria that are particularly important for the military environment and for operation with a mix of users indicated that FDMA performs much better than past analyses had shown. With the same satellite power and RF bandwidth, FDMA was found to offer nearly as much satellite throughput as TDMA and considerably more than SSMA.

The report consists of three volumes. Volume One provides a summary of the study which includes a description of the analysis approach, documentation of the pertinent equations, numerical results, and conclusions. Detailed analysis and investigation of the problem areas, as well as derivations of analytical expressions, are contained in the appendices in Volume Two. Volume Three provides a technical assessment of the suitability of PSK/FDMA for operation with a mix of users and compares its performance with other multiple-access alternatives, in particular, with that of time-division multiple access (TDMA) and spread-spectrum multiple access (SSMA).